SHALLOW-SEISMIC SITE CHARACTERIZATIONS OF NEAR-SURFACE GEOLOGY AT 20 STRONGMOTION STATIONS IN WASHINGTON STATE

Final Technical Report

USGS/NEHRP Award Number G09AP00021

By

Recep Cakir
Washington Department of Natural Resources
Division of Geology and Earth Resources
MS 47007, Olympia, WA 98504-7007
Phone: (360) 902-1460, Fax: (360) 902-1785
Email: recep.cakir@dnr.wa.gov

and

Timothy J. Walsh
Washington Department of Natural Resources
Division of Geology and Earth Resources
MS 47007, Olympia, WA 98504-7007
Phone: (360) 902-1432, Fax: (360) 902-1785
Email: tim.walsh@dnr.wa.gov

CONTENTS

FIGURES

TABLES

Shallow-Seismic Site Characterizations of Near-Surface Geology at 20 Strongmotion Stations in Washington State

Recep Cakir and Timothy J. Walsh
Washington Division of Geology and Earth Resources
MS 47007; Olympia, WA 98504-7007

ABSTRACT

In this NEHRP-funded study, we conducted shallow seismic surveys, including Multichannel Analysis of Surface Waves (MASW), Microtremor Array Measurements (MAM), and P- and S-wave refraction methods to estimate near-surface P- and S-wave velocity (Vp and Vs) profiles at 20 Pacific Northwest Seismic Network (PNSN) strongmotion sites in Washington. We subsequently calculated Vs30m (average Vs in the top 30 m), as well as Vp/Vs and Poisson's Ratio profiles, from the measured Vp and Vs. We provide these quantities in tabular form for each site. Specific to this study, we also prepared geological information for the 20 sites. Results can be directly used to analyze site responses at 20 strongmotion stations and to modify local and regional shake map preparations in Washington.

INTRODUCTION

The Washington State Department of Natural Resources (DNR), Division of Geology and Earth Resources (DGER), conducted shallow seismic surveys, including Multichannel Analysis of Surface Waves (MASW), Microtremor Array Measurements (MAM), and P- and S-wave refraction methods to estimate near-surface P- and S-wave velocity (Vp and Vs) profiles at 20 Pacific Northwest Seismic Network (PNSN) strongmotion sites in Washington. Work was funded through the U.S. Geological Survey/National Earthquake Hazard Reduction Program external grant program (USGS/NEHRP Award Number G09AP00021).

Puget Sound, Washington, and the coastal areas of Oregon, Washington, and British Columbia, Canada, are historically the most seismically active regions in the Pacific Northwest (Wong and others, 2003; Pratt and others, 2003; Atwater, 1996). The damaging interslab 1949 Olympia (M=7.1), 1965 Seattle-Tacoma (M=6.5), and 2001 Nisqually (M=6.8) earthquakes are recent examples of the region's seismic activity. A Cascadia subduction megathrust earthquake (M=9) (Atwater, 1996) can be expected in the not too distant future.

Immediately after a large earthquake, emergency managers need to assess the most and least damaged areas. The U.S. Geological Survey Earthquake Hazards Program (USGS-EHP) developed the ShakeMap, providing necessary near-real-time maps of ground motion and shaking intensity following significant earthquakes. The accuracy of rapid post-earthquake ground motion products, such as ShakeMap and ShakeCast, depends on the correct estimation of the effects of local shallow soils on recorded ground motions. However, many of the PNSN-monitored seismograph sites in Washington and Oregon have no measurements of shallow seismic velocities, which is an accurate way of assessing the site response. At sites for which shallow seismic velocities are available, necessary corrections on the observed ground motion data are easy to make (Paul Bodin, PNSN, oral commun., 2009).

The current NEHRP site class map (Palmer and others, 2004) of Washington State was constructed based on the seismic refraction shear-wave data acquired on each geologic unit. Then NEHRP site classes associated with uncertainties (types A through E), based on the top 30-m averaged shear-wave velocities (A=hard rock site [Vs_{30m} > 1,500 m/sec] through E=soft clays [Vs_{30m}<180 m/sec]) (Borcherdt, 1994), cannot be used as direct information at strong motion station sites. Therefore, it is very important that strong motion sites must be carefully

characterized to reduce the uncertainties on the recorded ground motions and relative amplifications incorporated in the probabilistic seismic hazard mapping procedure (Frankel and others, 2007). A clear understanding of the non-linear amplification effect at soil sites is one of the most important part of the site specific seismic hazard mapping (Aki, 1993), particularly in and around the metropolitan areas such as Seattle, WA.

In order to accurately quantify the near-surface seismic properties (Vs=shear-wave velocity, Vp=P-wave velocity, and Poisson's Ratio) with respect to depth, we conducted noninvasive active and passive surveys at 20 station sites in Washington (Fig. 1). We then calculated Vs from 1) active-source (8.2 kg sledgehammer) MASW surface wave (Rayleigh wave) data or S-wave refraction data, and 2) passive-source MAM (noise correlation) data. Also, we calculated the Vp from the active-source P-wave refraction data. We used additional downhole seismic data from Wong et al. (2010) and Cakir et al. (2008) in the Vs and Vp data analysis for station sites BSFP, KCAM, and WISH. Station sites HART and ALKI characterized previously by Wong et al. (2003) and Williams et al. (1999) were also surveyed. Finally, we collected all available nearby geotechnical and well log reports for each station site, and briefly reevaluated site geology.

In addition, we ran seismic surveys as a demonstration for K-12 students at few station sites located on school property. It was an educational exercise that was highly appreciated by the school principals and teachers and by the excited students who for the first time experienced generating and observing ground vibration signals. We always gave brief information to site owners (private, school principals, fire station managers, etc.) about our site characterization study and the funding agency, and explained importance of this research for their building and built environment.

We published a Seismological Society of America (SSA) abstract (Cakir and others, 2010) from this work and are working on a paper to be published in a relevant refereed journal, and internal report describing the project data and results to be posted on the Department of Natural Resources (DNR) website. Maps on the interactive mapping site will be linked to raw seismic data and the report. Finally, we prepared the project results and information for the strong motion sites descriptions to be posted on the Pacific Northwest Seismic Network (PNSN) website (http://www.pnsn.org).

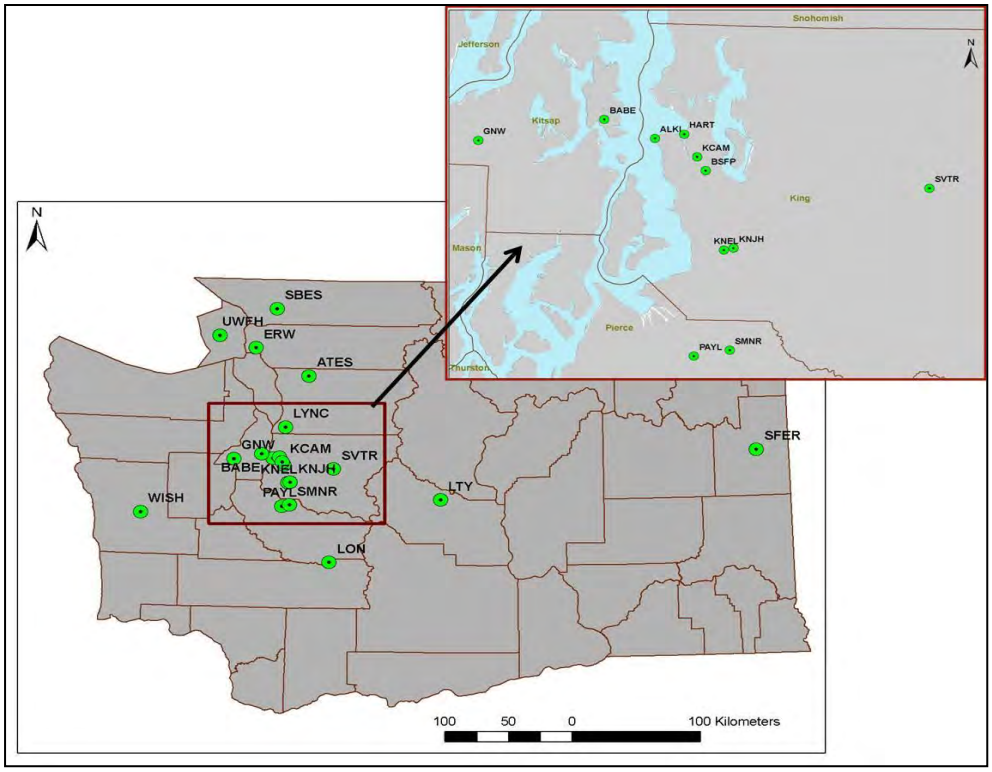

Figure 1. Shallow seismic survey locations.

GEOLOGIC SETTING

ALKI

This site is underlain by a thin (<.5m) veneer of loose sediment overlying the Blakeley Formation of Weaver (1916) as redefined by Fulmer (1975). Exposures within 100 m to the east and west of this site are fine- to medium-grained micaceous sandstone interbedded with siltstone, probably representing the Restoration Point Member of Fulmer (1975). The rocks here strike WNW and dip steeply (70-80°) to the north (Waldron, 1967).

ATES

The sediments underlying this site were mapped as the Arlington Gravel Member of the Vashon Drift (Minard, 1985). Dragovich and others (2004) map latest Pleistocene alluvial fans on this surface and Dragovich (Washington Division of Geology and Earth Resources, oral commun., 2010) identified thin (<2 m) laharic deposits of the White Chuck assemblage of Beget (1981) commonly present on this surface. Exposure at this site is insufficient to observe the fine detail of the geology.

BABE

This site is underlain by Vashon Till. Blakely Harbor Formation of Fulmer (1975) is exposed along the ridge a short distance to the southeast (Haugerud, 2005) and is probably present at a shallow depth beneath the till.

BSFP

This site is underlain by Holocene alluvium of the Duwamish River. The Duwamish Valley was an arm of Puget Sound after the retreat of the Puget Lobe at the end of the Fraser Glaciation and was infilled rapidly by sediment largely derived from Mount Rainier (Dragovich and others, 1994). Identification of the ~5,600-year-old Osceola mudflow at a depth of ~81 m below sea level a few miles south of this site suggests deposition of more than 90 m of alluvium over the last 5,000 years. These sandy sediments are therefore loose to very loose and are liquefiable. During the 2001 Nisqually earthquake, numerous sand blows erupted through the nearby runway at Boeing Field (Troost and others, 2001).

ERW

This site is underlain by the Jurassic Fidalgo Complex meta-intrusive rocks of Mount Erie (Dragovich and others, 2000), mostly metagabbro and metadiorite here. A dacite dike intrudes the complex at the north end of our seismic line, about 30 m north of the strongmotion instrument.

GNW

This site is shown on the 1:100,000-scale map as underlain by gabbro, but subsequent, more detailed mapping (Clark, 1989; Haeussler and Clark, 2000) show this site to be underlain by Eocene felsic plutonic rocks—quartz monzonite, quartz diorite, and tonalite. It is also very close to an exposure of the trace of the Green Mountain fault.

HART

This site is underlain by fill placed on tide flat deposits. Assuming that the tide flat was at about mean sea level, the fill is probably about 3 to 5 m thick. This site is liquefiable, as evidenced by the sand blow that erupted adjacent to the instrument during the 2001 Nisqually earthquake. An account of that sand blow, which was witnessed by Bob Norris (USGS) can be found at http://spike.geophys.washington.edu/SEIS/EQ_Special/WEBDIR_01022818543p/quakestory.html.

KCAM

This site is underlain by Holocene alluvium of the Duwamish River. The Duwamish valley was an arm of Puget Sound after the retreat of the Puget Lobe at the end of the Fraser Glaciation and was infilled rapidly by sediment largely derived from Mount Rainier (Dragovich and others, 1994). Identification of the ~5,600 year-old Osceola mudflow at a depth of ~80 m below sea level (Luzier, 1969) a few miles south of this site suggests deposition of more than 90 m of alluvium over the last 5,000 years. These sandy sediments are therefore loose to very loose and are liquefiable. During the 2001 Nisqually earthquake, numerous sand blows erupted through the nearby runway at Boeing Field (Troost and others, 2001).

KNEL

This site is underlain by Holocene alluvium of the White/Duwamish River. The Osceola mudflow is present at a depth of ~80 m below sea level approximately 1 mi southwest of this site, suggesting deposition of more than 90 of alluvium over the last 5,000 years. These sandy sediments are therefore loose to very loose and are liquefiable.

KNJH

This site is underlain by Holocene alluvium of the White/Duwamish River. The Osceola mudflow is present at a depth of ~80 m below sea level approximately 1 mi southwest of this site, suggesting deposition of more than 90 m of alluvium over the last 5,000 years. These sandy sediments are therefore loose to very loose and are liquefiable.

LON

This site is underlain by Oligocene volcanic breccia, volcaniclastic sandstone, and tuffaceous siltstone of the Ohanapecosh Formation (Fiske and others, 1963).

LTY

This site is underlain by thin- to very thick-bedded, cross-bedded feldspathic sandstone interbedded with carbonaceous mudstone of the Swauk Formation (Taylor, 1985). The beds dip shallowly to the west here along the crest of a west-plunging anticline. Numerous basalt dikes of the Teanaway dike swarm intrude the Swauk in the vicinity, but there did not appear to be any dikes within about 300 m of the instrument.

LYNC

This site is underlain by a broad ground moraine of Vashon Till (Minard, 1983). Till thickness is variable but commonly on the order of 10 m thick with a thin (<1 m) veneer of loose sand and gravel.

PAYL

This site is underlain by alluvium of the Puyallup River (Troost, in review) and is very close to the edge of the ancient Puyallup delta (Dragovich and others, 1994). The Osceola mudflow, which defines this delta in the subsurface, underlies the site at a depth of about 12 m, so the alluvium underlying this site is younger than about 5,700 years. Also underlying this site is ~2,300-year-old laharic sand from Mount Rainier that was associated with a sand blow from the 1949 earthquake very close to this school (Palmer and others, 1991).

SBES

This site is underlain by the Padden Member of the Eocene Chuckanut Formation (Johnson, 1982; Lapen, 2000), which consists of sandstone, conglomerate, mudstone, and minor coal. Bedrock is poorly exposed in the vicinity of the school but is fine-grained sandstone where visible. There are variable amounts of fill supporting the foundation of the building, probably less than 1.5m. Maintenance staff at the school confirmed that the building is founded on bedrock directly under the instrument.

SFER

This site is underlain by a thin veneer of sandy Missoula flood deposits over the Priest Rapids Member of the Wanapum Basalt, Columbia River Basalt Group (Derkey and others, 1999).

SMNR

This site is underlain by Holocene alluvium of the Puyallup River (Crandell, 1963). The depth to the Osceola mudflow here is about 9 m, and the total thickness of Holocene alluvium is about 200 ft (Dragovich and others, 1994).

SVTR

This site is underlain by Quaternary alluvium of the Snoqualmie River (Dragovich and others, 2009). The cross section from Dragovich and others (2009) infers the thickness of alluvium to be about 23 to 30 m overlying Vashon Till in the vicinity of the school.

UWFH

This site is underlain by volcaniclastic metasiltsone and metasandstone of the middle member of the Mesozoic Constitution Formation (Vance, 1975; Brandon and others, 1983). Bedrock is well exposed on the seaward side of the building housing the instrument, but the soil thickens landward. Massive metasiltstone is exposed on the southeast side of the building and metasandstone is exposed in the beach below.

WISH

This site is underlain by alpine glacial outwash sand and gravel (Mobray drift of Carson, 1970) composed of sandstone and basalt derived from the core of the Olympic Mountains. Clasts are generally moderately to well rounded, with characteristic red-orange weathering rinds. Soil is deeply weathered to depths exceeding 3.5 m (Logan, 2003). Our borehole at the site removed orange-brown gravel with varying amounts of sand and silt.

SEISMIC SURVEY AND DATA PROCESSING METHODS

Multichannel Analysis of Surface Waves (MASW)

This method has been extensively studied and tested for various shallow earth problems by the Kansas Geological Survey (KGS) (Miller and others, 1999; Park and others, 1999; Xia and others, 2000). More applications and references can found at the KGS website (http://www.kgs.ku.edu/ Geophysics/pubs.html). An 8.2 kg sledgehammer source and 4.5-Hz vertical geophones with (generally) 3 m interval were used to generate and receive surface (Rayleigh) waves recorded on a 24-channel seismograph (GEODE). Time sampling, record length, and shot interval for MASW acquisition and geometry were generally selected as 0.125 millisecond, 1 second, and 3 meters, respectively. Dispersion curves (phase velocity vs. frequency) and their inverted shear-wave velocity profiles were obtained by using procedure described in the SeisImager/SW software manual (Geometrics, 2006). Figure 2 shows the general processing steps of the 1D/2D MASW analysis (Geometrics, 2006). Figure 3 shows a flow chart of two-dimensional MASW processing steps.

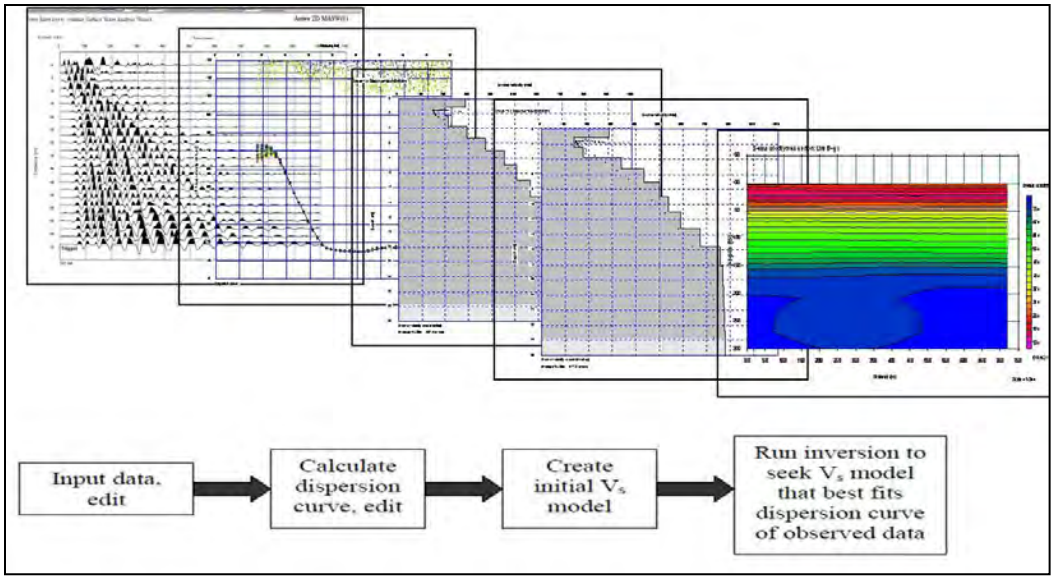

Figure 2. General steps of the 1D/2D Multichannel Analysis of Surface Waves (MASW) (Geometrics, 2006).

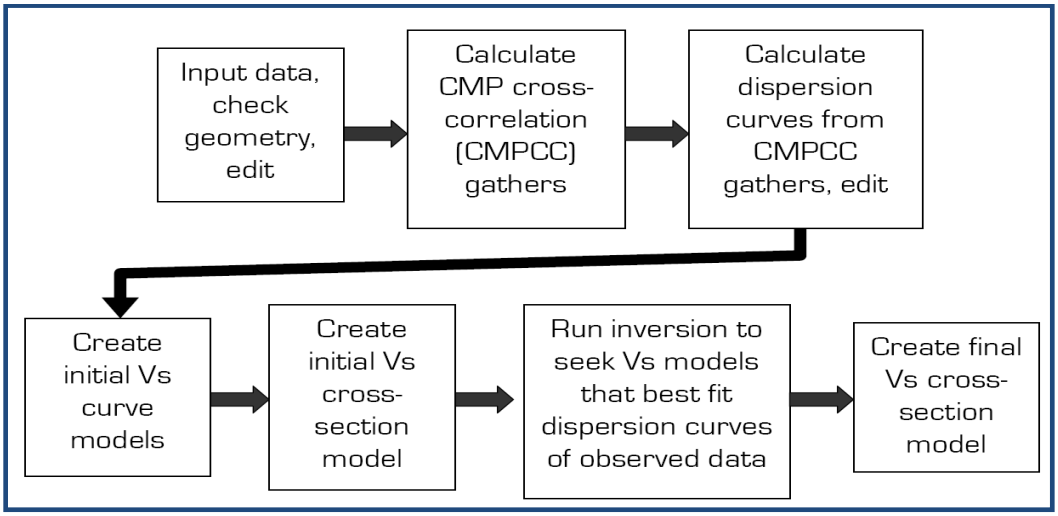

Figure 3. 2D imaging processing steps for the MASW data (Underwood, 2007).

Microtremor Array Measurements (MAM)

We recorded passive-source vibrations generated by cultural noise, traffic, wind, etc. We considered steady vibrations, examples given in Geometrics (2006), as the best quality data. The MAM field data acquisition parameters of 2-millisecond sampling time, 32-second record length, and linear (a line) or L-shape geometry were commonly used. Geophone array geometry (linear or L-shaped) was selected depending on the availability of the cultural and natural noises near the sites (Geometrics, 2006), and on where space permitted. To determine a full stretched dispersion curve (for example, 4–50Hz); dispersion curves of active (MASW) and passive (MAM) surface-wave methods were combined to better estimate deeper (>15 or 30 m) and shallow (<15 or 30 m) shear-wave velocities. Due to seismic-source energy limitation (lack of penetration to deeper depths by the sledge hammer blows) and short geophone spread length (maximum 115 m), these two dispersion curves were combined in most instances.

Figure 4 shows a full field survey setup of the MAM and its data recording scheme: passive seismic sources, such as local natural and manmade vibrations, interact with local near-surface geology under an array (linear or circular) of sensors transmitting the vibration signals to a recorder, having an Ethernet connection to a laptop that displays and stores the recorded digital seismic signals. A 10-minute recording for a 24-channel linear array was made by repeating the 32-second recording 20 times. This total 10-minute recording is long enough to capture characteristic vibrations of passive local seismic sources interacting with near-surface geology under the survey sensor arrays (linear, L-shaped or circular) (Fig. 4). Depending on site conditions, we generally choose maximum geophone spread lengths (indication for the maximum target depth) of 48, 69 or 115 m for the linear array and of 30 or 50 m for the L-shaped array. Due to limitations of the low-frequency passive seismic sources availability, this maximum depth was not reached at a few station sites. However, generally soil Vs profiles of the top 30 m were well determined using combined passive and active dispersion curves. The passive method estimates the Vs better for deeper parts of the soil, whereas the active method better resolves the shallower parts. Figure 5 shows the processing steps for the MAM data.

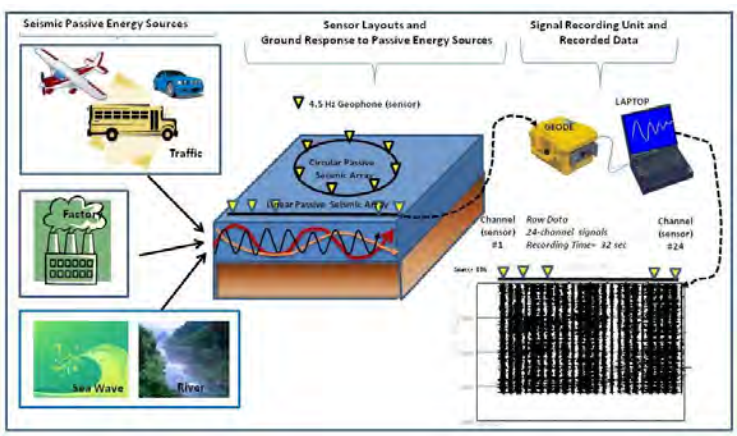

Figure 4. A schematic view for Microtremor Array Measurement (MAM) passive seismic survey and its data (duration=32 seconds) on a 24-channel seismograph (Geode seismograph, Geometrics Inc.); passive seismic signals consisting of cultural and natural noise propagating at various wavelengths (sampling different layered materials) interact with near-surface geology under linear and circular sensor arrays. The seismograph receives signals from the sensor array and transfers them to the laptop as a digital signal. An example record of a 32-second 24-channel passive survey (MAM) data set is shown (bottom-right corner).

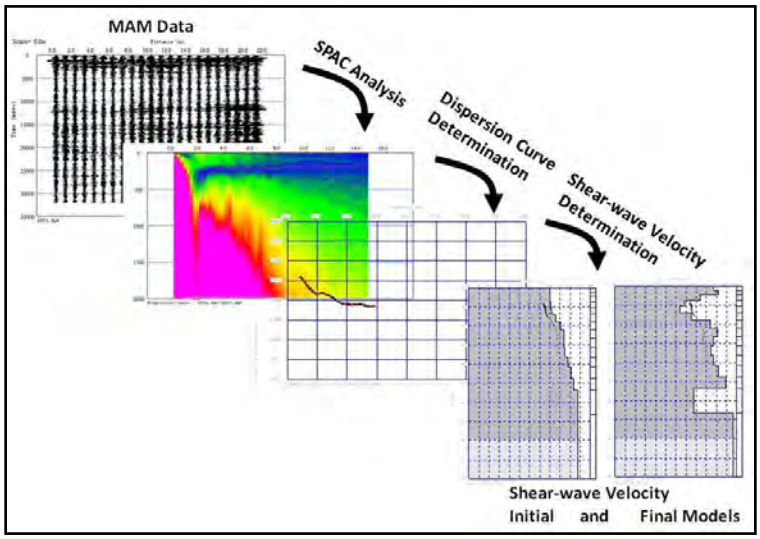

Figure 5. Microtremor Array Measurement (MAM) processing steps: The MAM data having a total of 10 minutes of approximately 20 32-second passive seismic records are used as input for Spatial Autocorrelation (SPAC) analysis, resulted in a dispersion (frequency vs. velocity) image edited for the best and most reasonable construction of the dispersion curve. Then a 1D shear wave velocity (Vs) profile is calculated from the dispersion curve. A final Vs profile is generated after an inversion process. The Vs velocity profile represents the middle part of the array (for example, middle section of the linear or an L-shaped array).

S- and P-Wave Refraction

We recorded active-source (sledgehammer) shear wave data using 24 14-Hz horizontal-component geophones generally spaced 2-3 m apart, with the exception of the ALKI station site where we used 1 and 1.5 m geophone intervals. Forward and reverse shots (minimum two, generally from both ends of the seismic line) were performed, where space permitted, to account for possible dipping of sub-layers. We used 0.0625 to 0.250 milliseconds time intervals, which were determined after test shots were performed to make sure SH-wave doublets (Fig. 6) were fully covered on 24 channels. In general, we set time intervals to lower sampling (oversampling) rates and record length to a longer recording time (1–2 seconds) covering full waveforms, including SH and Love waves.

A 9-ft-long 6 x 10 in. wood beam with 1.5-in.-thick protective steel end caps was coupled to the ground by parking the front two wheels of the field vehicle on top of the beam. We generated horizontally polarized, out-of-plane shear waves (SH) by striking each end of the wood beam with an 8.2-kg sledgehammer. These shear wave energy signals were then received by 24 14-Hz horizontal geophones and recorded on a 24-channel Geode seismograph, manufactured by Geometrics Inc. Figure 6 shows an example of the S-wave data acquired in this study.

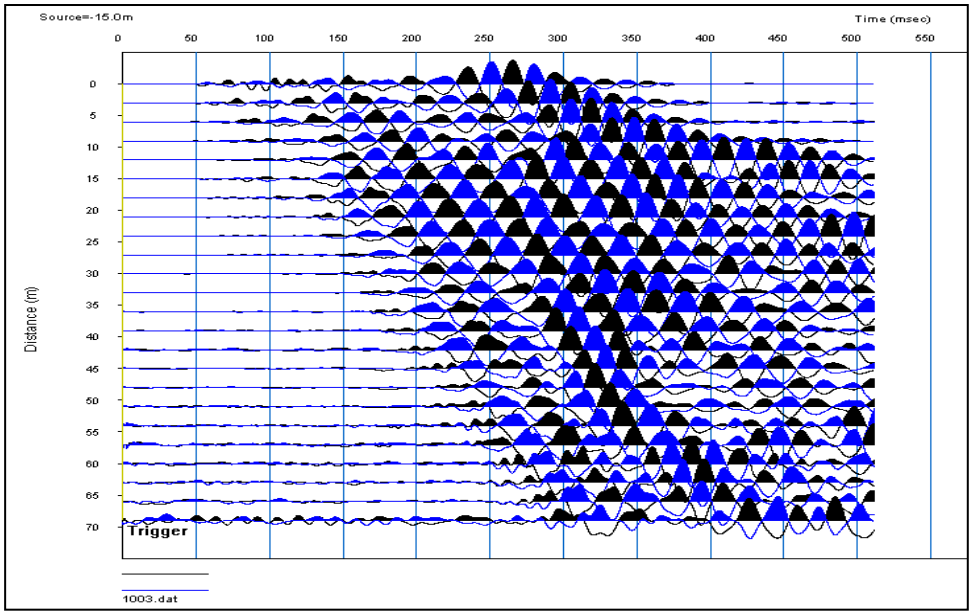

Figure 6. A shot gather with 180°-polarized shear-wave onsets, generated by striking both ends of the wood beam coupled to the ground by parking the front two wheels of the field vehicle on the beam. First onset of the doublets show the arrival times picked for refraction analysis.

We also generated P-wave data by vertically striking an aluminum plate with an 8.2-kg sledgehammer and recorded them on 4.5-Hz vertical component geophones at about 3-m spacing. We generally used the same S-wave linear array geometry and recording parameters (geophone spacing, record length, spread length, time interval) for the in-plane P-wave surveys, as well as a large part of the active surface (Rayleigh) wave linear array parameters. Figure 7 shows a P-wave shot gather and P-wave first arrivals picked and connected (red line) indicating presence of two layers.

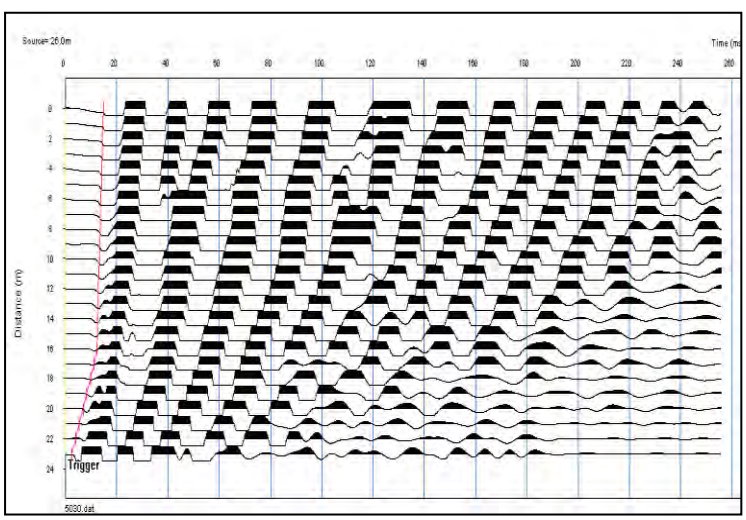

Figure 7. An example of P-wave shot gather. Red line marks the first arrivals of P waves at each geophone location. These first arrival picks were later used for a simple two- or three-layer time-term inversion analysis.

We used a ―time-term inversion" calculation method for a simple three-layer refraction model (Geometrics, 2009). After calculation of the velocity model from the travel time curves, a ray tracing was run and initial model generated for the tomography, resulting in a final layered model. Figure 8 shows the steps of the data analysis of the time-term inversion.

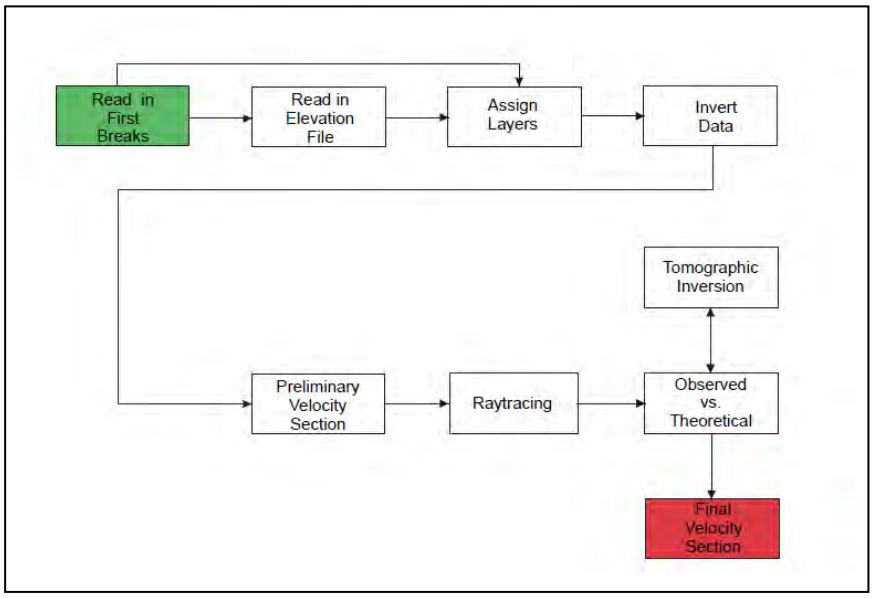

Figure 8. The general flow of the time-term inversion technique (Geometrics, 2009). To estimate Vp and Vs; a) first-arrival times were picked from the shot gathers and travel-time curves generated from these picks, b) preliminary velocity section were obtained after inverting the travel times curves whose layers visually assigned, c) initial travel time curves were later modified based on running the raytracing, finally d) nonlinear travel time tomography was iteratively run to find the final model until travel time data fits the perturbed initial model (Zhang and Toksöz, 1998).

SEISMIC SITE CHARACTERIZATION RESULTS

Processed active (MASW and S- and P-wave refraction) and passive (MAM) source or a combination of MASW and MAM survey data reached depths ranging from 30 to 65 m. The estimated Vs and Vp profiles for top 30 m of ground surface were used to calculate Vs30m values. Then the 20 strong motion sites were classified using the NEHRP site class categories, according to 2006 International Building Code (International Code Council, 2006, pages 303-304). Table 1 shows the 20 site names, their locations, types of seismic surveys, calculated Vs30m values, and classified site classes from this study. Site classes extracted from the statewide NEHRP site class map (Palmer and others, 2004) are also listed for comparison (Table 1). The estimated Vs and Vp and calculated Vp/Vs and Poisson's Ratio values are given in tabular forms along with the Vs, Vp and Vp/Vs plots in appendix A (Figs. A1 to A20).

Table 1. Shallow-seismic survey (strongmotion-station site) locations, conducted survey types, Vs30m which is the calculated average Vs to 30-m depth (International Code Council, 2006) and derived NEHRP site classifications from this study and from the current statewide NEHRP site class map for Washington (Palmer et al., 2004). S-wave refraction surveys were not run where sites were not suitable for a good geophone coupling to the ground (pavement area) or had a very noisy environment (such as station sites BSFP, KCAM and HART). We considered MASW, MAM and P-wave refraction as primary data acquisition methods for measurements of the Vs and Vp profiles (velocity versus depth).

Station Name	**Station Latitude (WGS84)**	**Station Longitude (WGS84)**	**Conducted Shallow Seismic Survey Methods**	**Vs30 (m/sec)**	**NEHRP Site Class (This study)**	**NEHRP Site Class (Palmer et al, 2004)**
ALKI	47.57510	-122.41760	MASW, MAM, Refraction (SH and P)	**784**	**B**	D
ATES	48.23617	-122.06042	MASW, MAM, Refraction (SH and P)	272	D	C-D
BABE	47.60637	-122.53586	MASW, MAM, Refraction (SH and P)	390	C	C
BSFP	47.52000	-122.29833	MASW, MAM, Refraction (P)	171	E	D-E, E
ERW	48.45383	-122.62634	MASW, MAM, Refraction (P)	1416	B	B
GNW_2	47.56411	-122.82496	MASW, MAM, Refraction (SH and P)	815	B	B
HART	47.58377	-122.35010	MASW, MAM, Refraction (P)	131	E	E
KCAM	47.54400	-122.31850	MASW, MAM, Refraction (P)	183	D	D-E
KNEL	47.38052	-122.25193	MASW, MAM, Refraction (SH and P)	183	D	D-E
KNJH	47.38454	-122.22957	MASW, MAM, Refraction (SH and P)	184	D	E
LON	46.74996	-121.80883	MASW, MAM, Refraction (SH and P)	662	C	B
LTY	47.25573	-120.66601	MASW, MAM, Refraction (P)	872	B	B
LYNC	47.82555	-122.29384	MASW, MAM, Refraction (P)	628	C	C
PAYL	47.19260	-122.31401	MASW, MAM, Refraction (SH and P)	165	E	D-E
SBES	48.76814	-122.41633	MASW, MAM, Refraction (P)	614	C	B
SFER	47.61944	-117.36651	MASW, MAM, Refraction (SH and P)	614	C	C
SMNR	47.20442	-122.23273	MASW, MAM, Refraction (SH and P)	160	E	D-E
SVTR	47.49576	-121.78159	MASW, MAM, Refraction (SH and P)	271	D	D-E
UWFH	48.54593	-123.01324	MASW, MAM, Refraction (P)	489	C	B
WISH	47.11698	-123.77118	Downhole, MASW, MAM, Refraction (P)	485	C	C

ACKNOWLEDGMENTS

We thank John Vidale, Paul Bodin, Lynn Simmons, and Bill Steele of the Pacific Northwest Seismic Network (PNSN) for kindly providing information and support to access the sites. Also, we wish to thank Christopher C. Maffucci, John Perreault, and Kaelen Burton for their generous contributions of time, effort, and enthusiasm during the field work and data processing. The authors thank our editor Jaretta M. Roloff for helpful suggestions on the layout and content of this report.

This research was supported by the U.S. Geological Survey, Department of the Interior, under USGS Award Number G09AP00021. The views and conclusions contained in this document are those of the authors and should not be interpreted as necessarily representing the official policies, either expressed or implied of the U.S. Government.

REFERENCES

Aki, Keiti, 1993, Local site effects on weak and strong ground motion: Tectonophysics, v. 218,, p. 93-111.

Atwater, B. F., 1996, Coastal evidence for great earthquakes in western Washington. *In* Rogers, A. M.; Walsh, T. J.; Kockelman, W. J.; Priest, G. R., editors, Assessing earthquake hazards and reducing risk in the Pacific Northwest: U.S. Geological Survey Professional Paper 1560, v. 1, p. 77-90. [http://pubs.usgs.gov/pp/p1560/p1560po.pdf]

Beget, J. E., 1981, Postglacial eruption history and volcanic hazards at Glacier Peak, Washington: University of Washington Doctor of Philosophy thesis, 192 p.

Borcherdt, R.D. 1994. Estimates of site-dependent response spectra for design (methodology and justification): Earthquake Spectra, v. 10, p. 617–653.

Brandon, M. T.; Cowan, D. S.; Muller, J. E.; Vance, J. A., 1983, Pre-Tertiary geology of San Juan Islands, Washington and southeast Vancouver Island, British Columbia: Geological Association of Canada Victoria Section Field Trip 5, 65 p.

Cakir, R; Walsh, T. J.; Contreras, T., 2008, Seismic and geotechnical site characterizations at four earthquake strong motion sites in Washington State: 21st SAGEEP Symposium, Proceedings, p. 1014-1025.

Cakir, R; Walsh, T. J.; Maffucci, C. M.; Perreault, J.; Burton, K., 2010, Shallow-seismic characterizations of near-surface geology at 20 strong-motion stations in Washington State: Seismological Research Letters, v. 81, no. 2, p. 382.

Carson, R. J., 1970, Quaternary geology of the south-central Olympic Peninsula, Washington: University of Washington Doctor of Philosophy thesis, 67 p., 4 plates

Clark, K. P., 1989, The stratigraphy and geochemistry of the Crescent Formation basalts and the bedrock geology of associated igneous rocks near Bremerton, Washington: Western Washington University Master of Science thesis, 171 p., 1 plate.

Crandell, D. R., 1963, Surficial geology and geomorphology of the Lake Tapps quadrangle, Washington: U.S. Geological Survey Professional Paper 388-A, 84 p., 2 plates. [http://pubs.er.usgs.gov/usgspubs/pp/pp388A]

Derkey, R. E.; Hamilton, M. M.; Stradling, D. F.; Kiver, E. P., 1999, Preliminary geologic maps of the Spokane NE and SE 7.5-minute quadrangles, Spokane County, Washington: Washington Division of Geology and Earth Resources Open File Report 99-6, 3 sheets, scale 1:24,000. [http://www.dnr.wa.gov/Publications/ger_ofr99-6_geol_map_spokanene_spokanese_24k.zip]

Dragovich, J. D.; DeOme, Alex J., 2006, Geologic map of the McMurray 7.5-minute quadrangle, Skagit and Snohomish Counties, Washington, with a discussion of the evidence for Holocene activity on the Darrington-Devils Mountain fault zone: Washington Division of Geology and Earth Resources Geologic Map GM-61, 1 sheet, scale 1:24,000, with 18 p. text. [accessed Jan. 6, 2010 at http://www.dnr.wa.gov/Publications/ger_gm61_geol_map_mcmurray_24k.zip]

Dragovich, J. D.; Pringle, P. T.; Walsh, T. J., 1994, Extent and geometry of the mid-Holocene Osceola mudflow in the Puget Lowland—Implications for Holocene sedimentation and paleogeography: Washington Geology, v. 22, no. 3, p. 3-26.

Dragovich, J. D.; Troost, M. L.; Norman, D. K.; Anderson, Garth; Cass, Jason; Gilbertson, L. A.; McKay, D. T., Jr., 2000, Geologic map of the Anacortes South and La Conner 7.5-minute quadrangles, Skagit and Island Counties, Washington: Washington Division of Geology and Earth Resources Open File Report 2000-6, 4 sheets, scale 1:24,000. [http://www.dnr.wa.gov/Publications/ger_ofr2000-6_geol_map_anacortess_laconner_24k.zip]

Dragovich, J. D.; Walsh, T. J.; Anderson, M. L.; Hartog, Renate; DuFrane, S. A.; Vervoot, Jeff; Williams, S. A.; Cakir, Recep; Stanton, K. D.; Wolff, F. E.; Norman, D. K.; Czajkowski, J. L., 2009, Geologic map of the North Bend 7.5-minute quadrangle, King County, Washington, with a discussion of major faults, folds, and basins in the map area: Washington Division of Geology and Earth Resources Geologic Map GM-73, 1 sheet, scale 1:24,000. [http://www.dnr.wa.gov/Publications/ger_publications_list.pdf]

Dragovich, J. D.; Wolfe, M. W.; Stanton, B. W.; Norman, D. K., 2004, Geologic map of the Stimson Hill 7.5-minute quadrangle, Skagit and Snohomish Counties, Washington: Washington Division of Geology and Earth Resources Open File Report 2004-9, 1 sheet, scale 1:24,000. [http://www.dnr.wa.gov/Publications/ger_ofr2004-9_geol_map_stimsonhill_24k.pdf

Fiske, R. S.; Hopson, C. A.; Waters, A. C., 1963, Geology of Mount Rainier National Park, Washington: U.S. Geological Survey Professional Paper 444, 93 p., 1 plate. [http://pubs.er.usgs.gov/usgspubs/pp/pp444]

Frankel, A. D.; Stephenson, W. J.; Carver, D. L.; Williams, R. A.; Odum, J. K.; Rhea, Susan, 2007, Seismic hazard maps for Seattle, Washington, incorporating 3D sedimentary basin effects, nonlinear site response, and rupture directivity. [http://pubs.usgs.gov/of/2007/1175/downloads/pdf/OF07-1175_508.pdf]

Fulmer, C. V., 1975, Stratigraphy and paleontology of the type Blakeley and Blakely Harbor Formations. *In* Weaver, D. W.; Hornaday, G. R.; Tipton, Ann, editors, Paleogene symposium and selected technical papers—Conference on future energy horizons of the Pacific coast: American Association of Petroleum Geologists Pacific Section, 50th Annual Meeting, p. 210-271.

Geometrics Inc., 2006, SeisImager/SW software manual—Windows software for analysis of surface waves: Geometrics Inc., p. 281.

Geometrics Inc., 2009, SeisImager/2D software manual; version 3.3, p. 257.

Haeussler, P. J.; Clark, K. P., 2000, Preliminary geologic map of the Wildcat Lake 7.5' quadrangle, Kitsap and Mason Counties, Washington: U.S. Geological Survey Open-File Report 00-356, 1 sheet, scale 1:24,000.

Haugerud, R. A., 2005, Preliminary geologic map of Bainbridge Island, Washington: U.S. Geological Survey Open-File Report 2005-1387, version 1.0, 1 sheet, scale 1:24,000. [http://pubs.usgs.gov/of/2005/1387]

International Code Council, 2006, International Building Code: International Code Council, Inc., 666 p.

Johnson, S. Y., 1982, Stratigraphy, sedimentology, and tectonic setting of the Eocene Chuckanut Formation, northwest Washington: University of Washington Doctor of Philosophy thesis, 221 p., 4 plates.

Lapen, T. J., 2000, Geologic map of the Bellingham 1:100,000 quadrangle, Washington: Washington Division of Geology and Earth Resources Open File Report 2000-5, 36 p., 2 plates, scale 1:100,000. [http://www.dnr.wa.gov/Publications/ger_ofr2000-5_geol_map_bellingham_100k.zip]

Logan, R. L., 2003, Geologic map of the Shelton 1:100,000 quadrangle, Washington: Washington Division of Geology and Earth Resources Open File Report 2003-15, 1 sheet, scale 1:100,000. [http://www.dnr.wa.gov/Publications/ger_ofr2003-15_geol_map_shelton_100k.pdf]

Luzier, J. E., 1969, Geology and ground-water resources of southwestern King County, Washington: Washington Department of Water Resources Water-Supply Bulletin 28, 260 p., 3 plates.

Miller, R. D.; Xia, J.; Park, C .B.; Ivanov, J., 1999, Multichannel analysis of surface waves to map bedrock: The Leading Edge, v. 18, no. 12, p. 1392-1396.

Minard, J. P., 1983, Geologic map of the Edmonds East and part of the Edmonds West quadrangles, Washington: U.S. Geological Survey Miscellaneous Field Studies Map MF-1541, 1 sheet, scale 1:24,000.

Minard, J. P., 1985, Geologic map of the Arlington East quadrangle, Snohomish County, Washington: U.S. Geological Survey Miscellaneous Field Studies Map MF-1739, 1 sheet, scale 1:24,000.

Palmer, S. P.; Pringle, P. T.; Shulene, J. A., 1991, Analysis of liquefiable soils in Puyallup, Washington. *In* Proceedings--Fourth International Conference on Seismic Zonation, Stanford, California, 1991: Earthquake Engineering Research Institute, v. 2, p. 621-628.

Palmer, S. P.; Magsino, S. L.; Bilderback, E. L.; Poelstra, J. L.; Folger, D. S.; Niggemann, R. A., 2004, Liquefaction susceptibility and site class maps of Washington State, by county: Washington Division of Geology and Earth Resources Open File Report 2004-20, 1 DVD [78 plates, 45 p. text]. [http://www.dnr.wa.gov/ResearchScience/Topics/GeologyPublicationsLibrary/Pages/pub_ofr04-20.aspx]

Park, C. B.; Miller, R. D.; Xia, J., 1999, Multi-channel analysis of surface waves, Geophysics, v. 64, no. 3, p. 800-808.

Pratt, T. L.; Brocher, T. M.; Weaver, C. S.; Creager, K. C.; Snelson, C. M.; Crosson, R. S.; Miller, K. C.; Trehu, A. M., 2003, Amplification of seismic waves by the Seattle basin, Washington State: Seismological Society of America Bulletin, v. 93, no. 2, p. 533-545.

Underwood, D., 2007, Introduction to SeisImager/SW, Geometrics Inc. (http://www.geometrics.com).

Taylor, S. B., 1985, Stratigraphy, sedimentology, and paleogeography of the Swauk Formation in the Liberty area, central Cascades, Washington: Washington State University Master of Science thesis, 199 p., 2 plates.

Troost, K. G., in review, Geologic map of the Puyallup 7.5-minute quadrangle, Washington: U.S. Geological Survey Miscellaneous Field Investigation, scale 1:24,000.

Troost, K. G.; Haugerud, R. A.; Walsh, T. J.; Harp, E. L.; Booth, D. B.; Steele, W. P.; Wegmann, K. W.; Pratt, T. L.; Sherrod, B. L.; Kramer, S. L., 2001, Ground failures produced by the Nisqually earthquake [abstract]: Seismological Research Letters, v. 72, no. 3, p. 396.

Vance, J. A., 1975, Bedrock geology of San Juan County. *In* Russell, R. H., editor, Geology and water resources of the San Juan Islands, San Juan County, Washington: Washington Department of Ecology Water-Supply Bulletin 46, p. 3-19.

Waldron, H. H., 1967, Geologic map of the Duwamish Head quadrangle, King and Kitsap Counties, Washington: U.S. Geological Survey Geologic Quadrangle Map GQ-706, 1 sheet, scale 1:24,000.

Weaver, C.E., 1916, The Tertiary formations of western Washington: Washington Geological Survey Bulletin, no. 13, 327 p.

Williams, R.A., W.J. Stephenson, A.D. Frankel, and J.K. Odum, 1999, Surface seismic measurements of near-surface P- and S- wave seismic velocities at earthquake recording stations, Seattle, Washington, Earthquake Spectra, v. 15, 565-584.

Wong, I.; Sparks, A.; Thomas, P.; Nemser, E., 2003, Evaluation of near-surface site amplifications in the Seattle, Washington, Metropolitan Area, Final Technical Report, U.S. Geological Survey, Award Number 00HQGR019.

Wong, I.; Stokoe, K.H.II; Cox, B.R.; Lin, Y.C.; Menq, F. Y., 2010, Geotechnical characterization and evaluation of site amplification at selected PNSN strong motion sites, Seattle, Washington, Final Technical Report, U.S. Geological Survey, Award Number 03HQGR0012.

Xia, J.; Miller, R.D.; Park, C.B., 2000, Comparing shear-wave velocity profiles from MASW with borehole measurements in unconsolidated sediments. Fraser River Delta, B.C., Canada: Jour. Environ. Eng Geophy. 5(3), 1-13.

Zhang, J. and Toksöz, M.N., 1998, Nonlinear refraction travel time tomography. Geophysics 63(5):1726-1737.

APPENDIX A. Tables for Vs, Vp, Vp/Vs and Poisson's Ratio values, and Plots for the Vs, Vp and Vp/Vs profiles in top 30 meters (Figures A1-A20)

ALKI

Depth Interval (m)		Vs (m/sec)
0.0	1.1	345.15
1.1	2.3	322.22
2.3	3.7	489.83
3.7	5.3	658.76
5.3	7.0	719.59
7.0	8.9	754.76
8.9	11.0	781.68
11.0	13.2	830.08
13.2	15.6	901.24
15.6	18.1	981.48
18.1	20.9	1024.33
20.9	23.7	1124.83
23.7	26.8	1162.00
26.8	30.0	1162.00

Depth Interval (m)		Vp (m/sec)
0.0	0.53	877.69
0.5	1.58	909.95
1.6	2.63	1020.07
2.6	3.68	1794.33
3.7	6.21	1899.14
6.2	8.73	2036.44
8.7	11.26	2108.45
11.3	13.78	2155.68
13.8	30.00	2169.61

Depth (m)	Vs (m/sec)	Vp (m/sec)	Vp/Vs	Poisson's Ratio
0	345.15	877.69	2.5	0.41
1	322.22	909.95	2.8	0.43
2	489.83	1020.07	2.1	0.35
3	489.83	1794.33	3.7	0.46
4	658.76	1899.14	2.9	0.43
5	719.59	1899.14	2.6	0.42
6	719.59	2036.44	2.8	0.43
7	754.76	2036.44	2.7	0.42
8	781.68	2036.44	2.6	0.41
9	781.68	2108.45	2.7	0.42
10	781.68	2108.45	2.7	0.42
11	830.08	2155.68	2.6	0.41
12	830.08	2155.68	2.6	0.41
13	901.24	2155.68	2.4	0.39
14	901.24	2169.61	2.4	0.40
15	901.24	2169.61	2.4	0.40
16	981.48	2169.61	2.2	0.37
17	981.48	2169.61	2.2	0.37
18	1024.33	2169.61	2.1	0.36
19	1024.33	2169.61	2.1	0.36
20	1024.33	2169.61	2.1	0.36
21	1124.83	2169.61	1.9	0.32
22	1124.83	2169.61	1.9	0.32
23	1124.83	2169.61	1.9	0.32
24	1162.00	2169.61	1.9	0.30
25	1162.00	2169.61	1.9	0.30
26	1162.00	2169.61	1.9	0.30
27	1162.00	2169.61	1.9	0.30
28	1162.00	2169.61	1.9	0.30
29	1162.00	2169.61	1.9	0.30
30	1162.00	2169.61	1.9	0.30

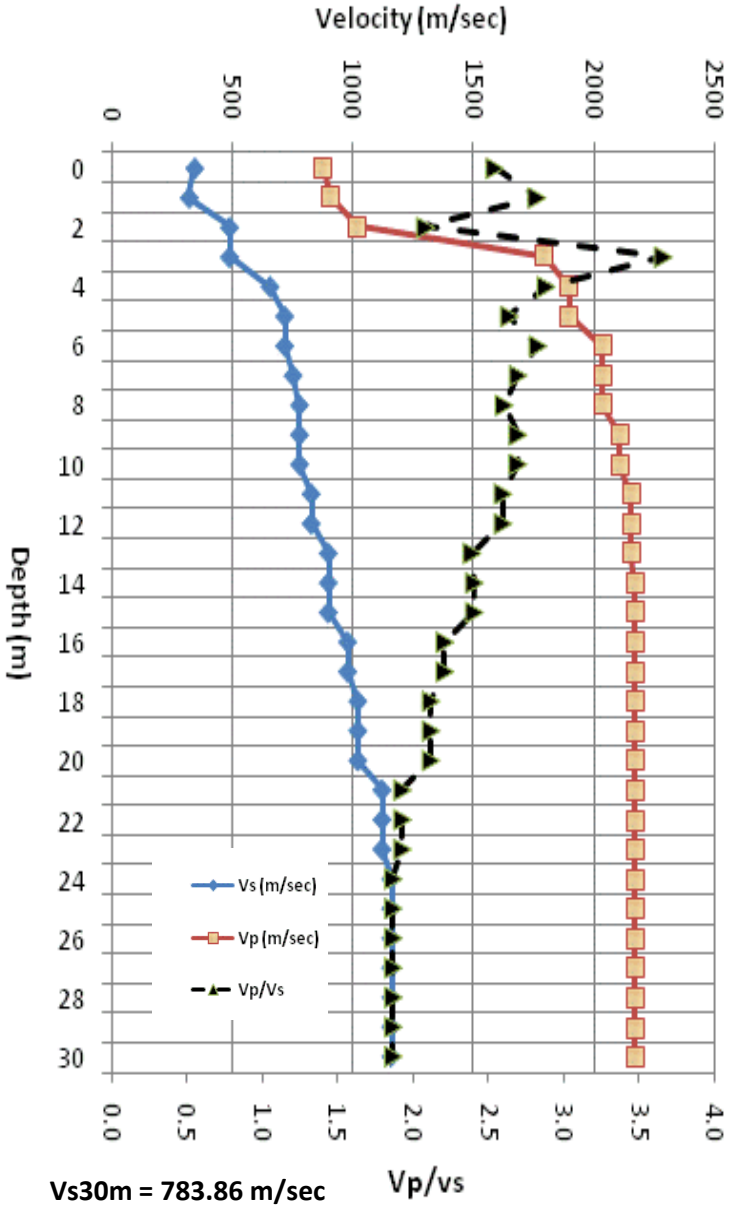

Vs30m = 783.86 m/sec

Figure A1. Vs, Vp, Vp/Vs and Poisson's Ratio profiles at ALKI .

ATES

Depth Interval (m)		Vs (m/sec)
0.0	1.1	176.72
1.1	2.2	209.87
2.2	3.5	220.61
3.5	4.9	225.71
4.9	6.4	243.86
6.4	8.1	275.99
8.1	9.8	288.77
9.8	11.7	288.85
11.7	13.7	281.22
13.7	15.8	270.02
15.8	18.0	263.76
18.0	20.4	266.21
20.4	22.8	281.90
22.8	25.4	310.18
25.4	28.1	343.51
28.1	30.9	380.39
30.9	33.8	397.26
33.8	36.8	420.65
36.8	40.0	427.45
40.0	-	427.45

Depth Interval (m)		Vp (m/sec)
0.0	0.6	365.17
0.6	1.9	367.50
1.9	3.2	367.64
3.2	4.5	367.64
4.5	5.8	698.99
5.8	7.1	1161.90
7.1	10.0	1208.80
10.0	12.9	1572.02
12.9	15.8	1806.76
15.8	18.7	1807.76
18.7	21.6	1839.72
21.6	24.5	1909.46
24.5	27.4	2055.98
27.4	30.4	2092.34
30.4	-	2092.34

Vs (m/sec)	Vp (m/sec)	Vp/Vs	Poisson's Ratio
176.72	365.17	2.1	0.35
209.87	367.50	1.8	0.26
220.61	367.64	1.7	0.22
220.61	367.64	1.7	0.22
225.71	367.64	1.6	0.20
243.86	698.99	2.9	0.43
275.99	1161.90	4.2	0.47
275.99	1208.80	4.4	0.47
288.77	1208.80	4.2	0.47
288.77	1208.80	4.2	0.47
288.85	1572.02	5.4	0.48
288.85	1572.02	5.4	0.48
281.22	1572.02	5.6	0.48
281.22	1806.76	6.4	0.49
270.02	1806.76	6.7	0.49
270.02	1806.76	6.7	0.49
263.76	1807.76	6.9	0.49
263.76	1807.76	6.9	0.49
266.21	1807.76	6.8	0.49
266.21	1839.72	6.9	0.49
281.90	1839.72	6.5	0.49
281.90	1839.72	6.5	0.49
281.90	1909.46	6.8	0.49
310.18	1909.46	6.2	0.49
310.18	1909.46	6.2	0.49
343.51	2055.98	6.0	0.49
343.51	2055.98	6.0	0.49
343.51	2092.34	6.1	0.49
380.39	2092.34	5.5	0.48
380.39	2092.34	5.5	0.48
380.39	2092.34	5.5	0.48

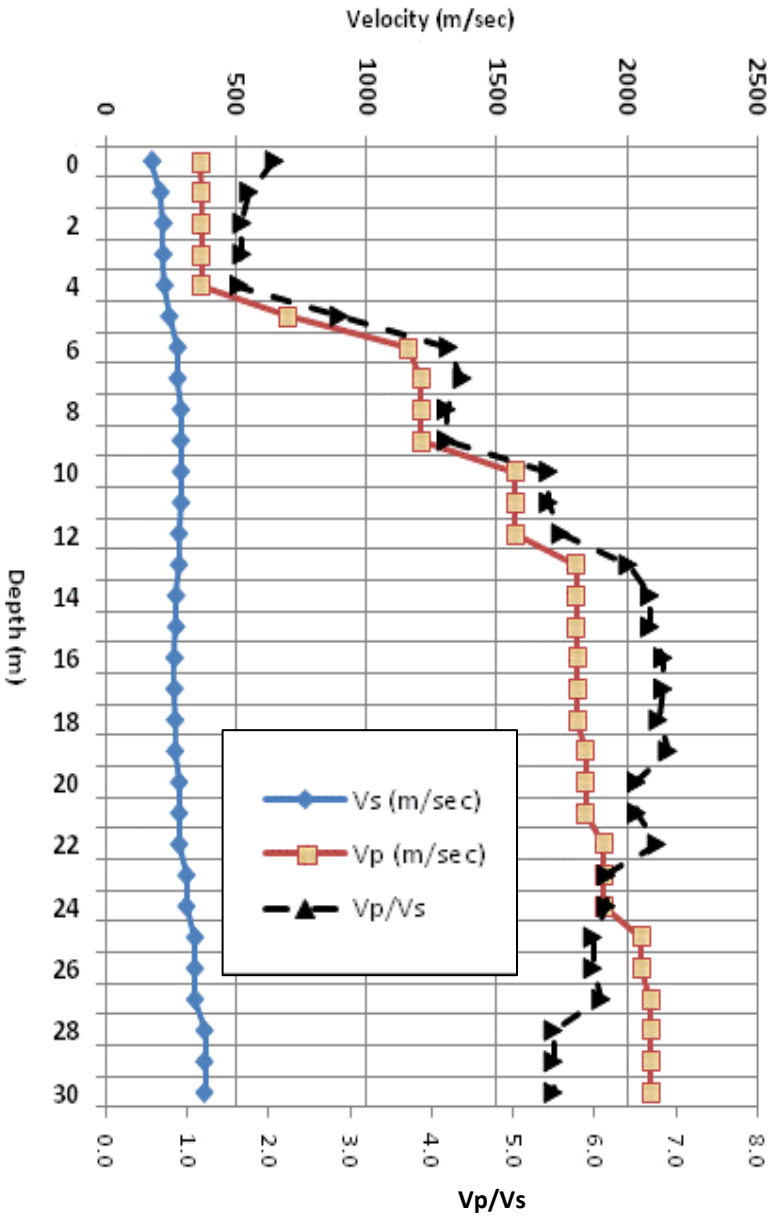

Vs30m = 272.00 m/sec

Figure A2. Vs, Vp, Vp/Vs and Poisson's Ratio profiles at ATES.

BABE

Depth interval (m)		Vs (m/s)
0.0	1.1	244.18
1.1	2.2	238.77
2.2	3.5	202.70
3.5	4.9	267.02
4.9	6.4	325.09
6.4	8.1	362.15
8.1	9.8	373.27
9.8	11.7	376.66
11.7	13.7	383.52
13.7	15.8	409.38
15.8	18.0	462.49
18.0	20.4	470.63
20.4	22.8	540.54
22.8	25.4	550.44
25.4	28.1	589.43
28.1	30.9	589.43
30.9	33.8	589.43
33.8	36.8	589.43
36.8	40.0	589.43
40.0	-	589.43

Depth Interval (m)		Vp (m/sec)
0.0	0.9	746.37
0.9	2.8	781.51
2.8	4.7	782.51
4.7	6.6	871.40
6.6	11.1	1124.76
11.1	15.6	1207.21
15.6	20.1	1588.68
20.1	24.6	1588.68
24.6	29.1	1588.68
29.1	-	1588.68

Depth (m)	Vs (m/sec)	Vp (m/sec)	Vp/Vs	Poisson's Ratio
0	244.18	746.37	3.1	0.44
1	238.77	781.51	3.3	0.45
2	202.70	781.51	3.9	0.46
3	202.70	782.51	3.9	0.46
4	267.02	782.51	2.9	0.43
5	325.09	871.40	2.7	0.42
6	362.15	871.40	2.4	0.40
7	362.15	1124.76	3.1	0.44
8	373.27	1124.76	3.0	0.44
9	373.27	1124.76	3.0	0.44
10	376.66	1124.76	3.0	0.44
11	376.66	1207.21	3.2	0.45
12	383.52	1207.21	3.1	0.44
13	383.52	1207.21	3.1	0.44
14	409.38	1207.21	2.9	0.44
15	409.38	1207.21	2.9	0.44
16	462.49	1207.21	2.6	0.41
17	462.49	1588.68	3.4	0.45
18	470.63	1588.68	3.4	0.45
19	470.63	1588.68	3.4	0.45
20	540.54	1588.68	2.9	0.43
21	540.54	1588.68	2.9	0.43
22	540.54	1588.68	2.9	0.43
23	550.44	1588.68	2.9	0.43
24	550.44	1588.68	2.9	0.43
25	589.43	1588.68	2.7	0.42
26	589.43	1588.68	2.7	0.42
27	589.43	1588.68	2.7	0.42
28	589.43	1588.68	2.7	0.42
29	589.43	1588.68	2.7	0.42
30	589.43	1588.68	2.7	0.42

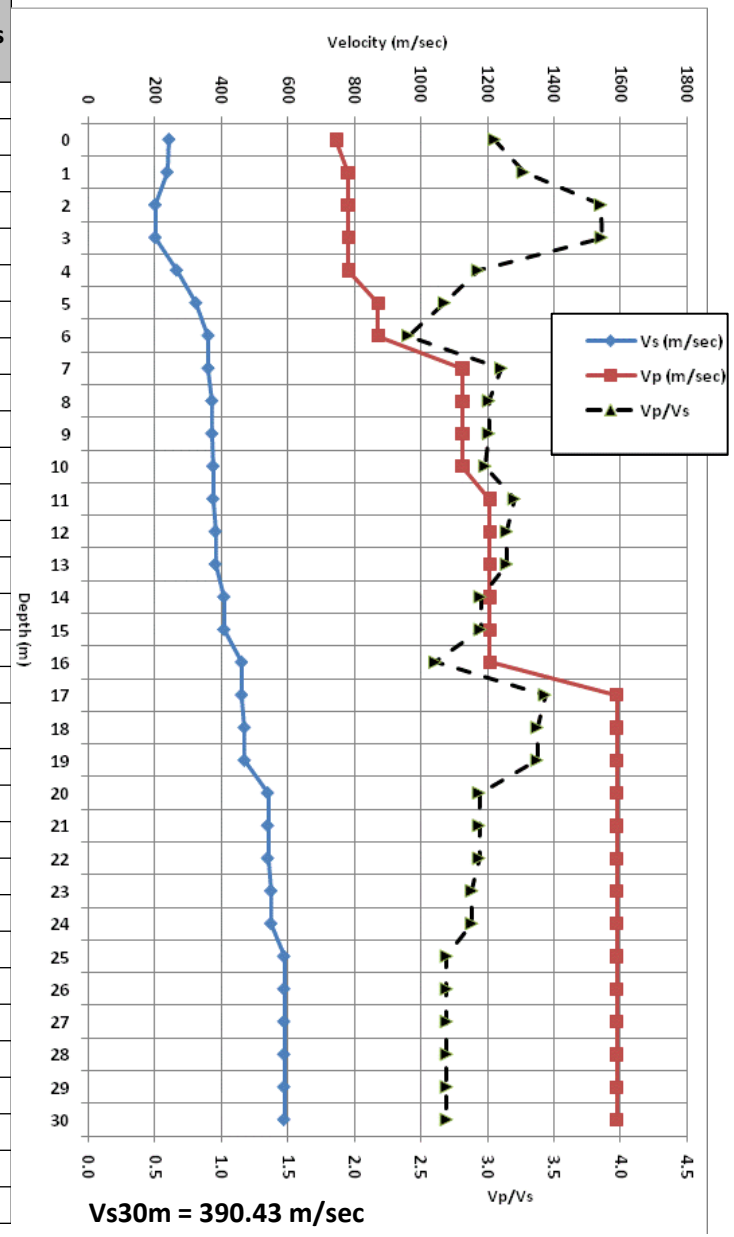

Vs30m = 390.43 m/sec

Figure A3. Vs, Vp, Vp/Vs and Poisson's Ratio profiles at BABE.

BSFP

Depth Interval (m)		Vs (m/sec)
0.0	1.1	154.20
1.1	2.2	151.36
2.2	3.5	148.41
3.5	4.9	146.80
4.9	6.4	145.69
6.4	8.1	149.71
8.1	9.8	155.12
9.8	11.7	159.77
11.7	13.7	164.01
13.7	15.8	166.24
15.8	18.0	166.38
18.0	20.4	171.90
20.4	22.8	184.63
22.8	25.4	201.74
25.4	28.1	219.13
28.1	30.0	222.40
30.0	33.8	222.40
33.8	36.8	222.40
36.8	40.0	222.40

Depth Interval (m)		Vp (m/sec) (Wong et al, 2003)
0.0	1.5	845.00
1.5	7.6	845.00
7.6	11.6	1541.00
11.6	15.2	1880.00
15.2	32.0	1420.00
32.0	40.5	1573.00
40.5	58.8	1306.00
58.8	61.9	1508.00
61.9	-	1899.00

Depth (m)	Vs (m/sec)	Vp (m/sec)	Vp/Vs	Poisson's Ratio
0	154.20	845.00	5.5	0.48
1	151.36	845.00	5.6	0.48
2	148.41	845.00	5.7	0.48
3	148.41	845.00	5.7	0.48
4	146.80	845.00	5.8	0.48
5	145.69	845.00	5.8	0.48
6	149.71	845.00	5.6	0.48
7	149.71	845.00	5.6	0.48
8	155.12	1541.00	9.9	0.49
9	155.12	1541.00	9.9	0.49
10	159.77	1541.00	9.7	0.49
11	159.77	1541.00	9.7	0.49
12	164.01	1880.00	11.5	0.50
13	164.01	1880.00	11.5	0.50
14	166.24	1880.00	11.3	0.50
15	166.24	1420.00	8.5	0.49
16	166.38	1420.00	8.5	0.49
17	166.38	1420.00	8.5	0.49
18	171.90	1420.00	8.3	0.49
19	171.90	1420.00	8.3	0.49
20	184.63	1420.00	7.7	0.49
21	184.63	1420.00	7.7	0.49
22	184.63	1420.00	7.7	0.49
23	201.74	1420.00	7.0	0.49
24	201.74	1420.00	7.0	0.49
25	201.74	1420.00	7.0	0.49
26	219.13	1420.00	6.5	0.49
27	219.13	1420.00	6.5	0.49
28	222.40	1420.00	6.5	0.49
29	222.40	1420.00	6.5	0.49
30	222.40	1420.00	6.5	0.49

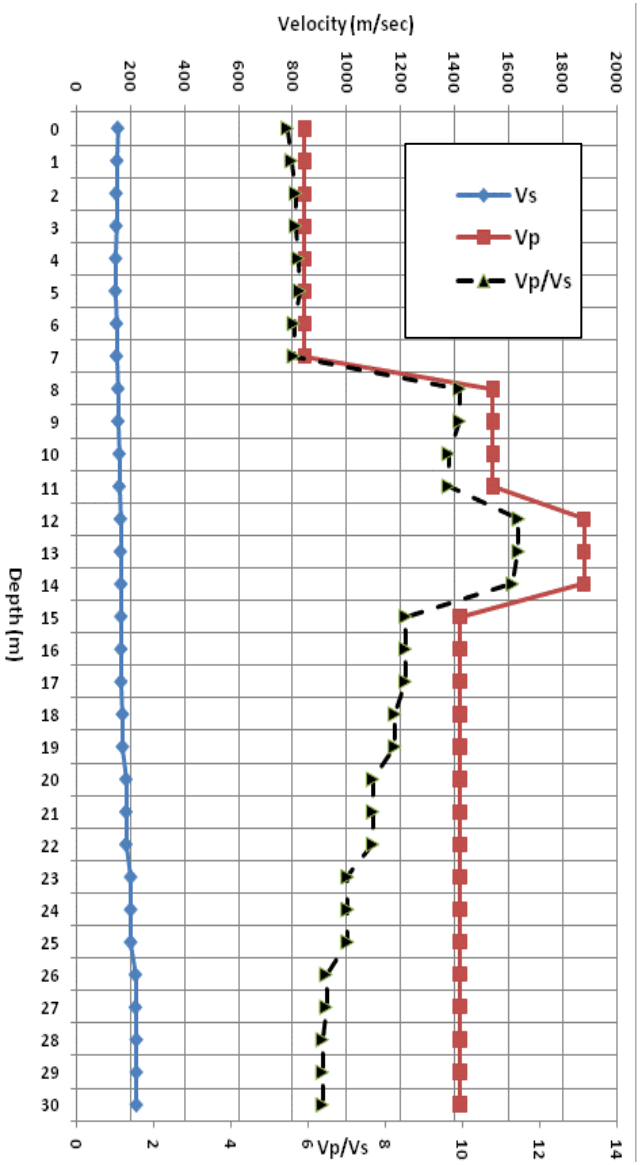

Vs30m=170.51 m/sec

Figure A4. Vs, Vp, Vp/Vs and Poisson's Ratio profiles at BSFP.

ERW

Depth Interval (m)		Vs (m/sec)
0.0	1.1	1230.15
1.1	2.2	1176.65
2.2	3.5	1084.92
3.5	4.9	1000.67
4.9	6.4	979.60
6.4	8.1	1001.32
8.1	9.8	1189.01
9.8	11.7	1265.07
11.7	13.7	1474.93
13.7	15.8	1719.05
15.8	30.0	1769.50

Depth Interval (m)		Vp (m/sec)
0.0	0.6	1188.57
0.6	1.8	1209.98
1.8	3.0	1232.34
3.0	4.2	1321.26
4.2	7.1	2133.93
7.1	10.0	2731.73
10.0	12.9	3099.48
12.9	15.8	3231.86
15.8	18.7	3238.56
18.7	30.0	3238.56
30.0	-	3238.56

Depth	Vs (m/sec)	Vp (m/sec)	Vp/Vs	PR
0.00	1230.15	2630.17	2.1	0.36
1.00	1176.65	2515.79	2.1	0.36
2.00	1084.92	2319.65	2.1	0.36
3.00	1084.92	2319.65	2.1	0.36
4.00	1000.67	2133.93	2.1	0.36
5.00	979.60	2133.93	2.2	0.37
6.00	1001.32	2133.93	2.1	0.36
7.00	1001.32	2731.73	2.7	0.42
8.00	1189.01	2731.73	2.3	0.38
9.00	1189.01	2731.73	2.3	0.38
10.00	1265.07	3099.48	2.5	0.40
11.00	1265.07	3099.48	2.5	0.40
12.00	1474.93	3099.48	2.1	0.35
13.00	1474.93	3231.86	2.2	0.37
14.00	1719.05	3231.86	1.9	0.30
15.00	1719.05	3231.86	1.9	0.30
16.00	1769.50	3238.56	1.8	0.29
17.00	1769.50	3238.56	1.8	0.29
18.00	1769.50	3238.56	1.8	0.29
19.00	1769.50	3238.56	1.8	0.29
20.00	1769.50	3238.56	1.8	0.29
21.00	1769.50	3238.56	1.8	0.29
22.00	1769.50	3238.56	1.8	0.29
23.00	1769.50	3238.56	1.8	0.29
24.00	1769.50	3238.56	1.8	0.29
25.00	1769.50	3238.56	1.8	0.29
26.00	1769.50	3238.56	1.8	0.29
27.00	1769.50	3238.56	1.8	0.29
28.00	1769.50	3238.56	1.8	0.29
29.00	1769.50	3238.56	1.8	0.29
30.00	1769.50	3238.56	1.8	0.29

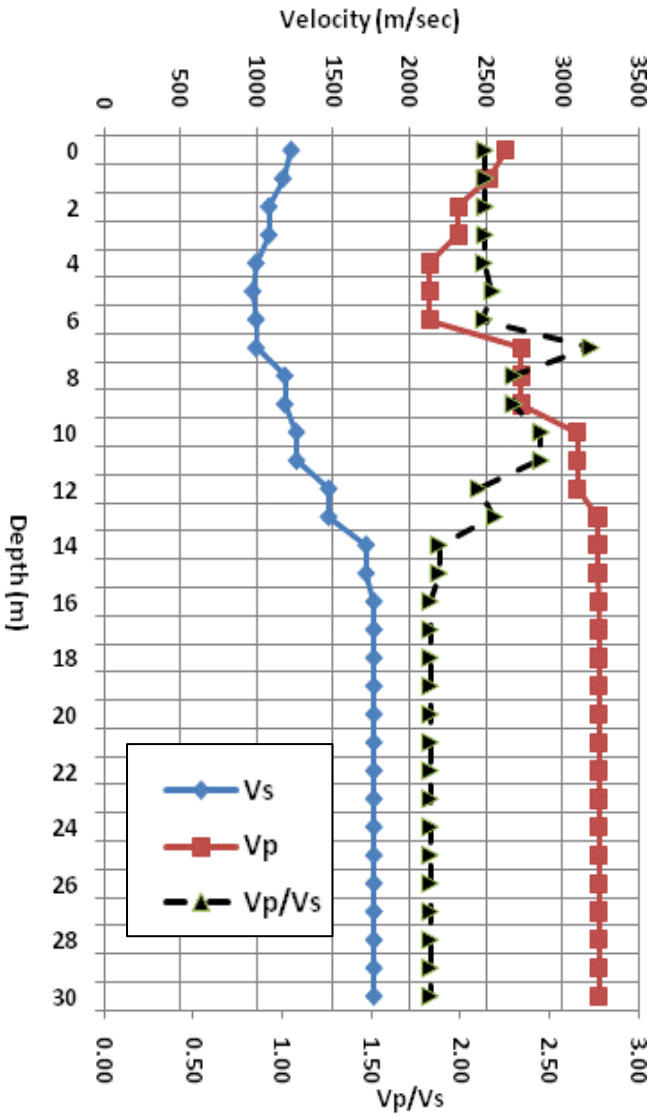

Vs30m=1416.18 m/sec

Figure A5. Vs, Vp, Vp/Vs and Poisson's Ratio profiles at ERW.

GNW_2

Depth Interval (m)		Vs (m/sec)
0.0	1.1	277.52
1.1	2.2	277.52
2.2	3.5	338.60
3.5	4.9	591.15
4.9	6.4	682.53
6.4	8.1	747.84
8.1	9.8	866.90
9.8	11.7	1018.39
11.7	13.7	1195.59
13.7	30.0	1286.93

Depth Interval (m)		Vp (m/sec)
0.0	0.7	625.47
0.7	2.1	625.47
2.1	3.3	625.87
3.3	4.6	1722.19
4.6	7.8	3290.67
7.8	10.9	3384.04
10.9	14.9	3384.04
14.1	30.0	3384.04

Depth (m)	Vs (m/sec)	Vp (m/sec)	Vp/Vs	Poisson's Ratio
0	277.5	625.47	2.3	0.38
1	277.5	625.47	2.3	0.38
2	338.6	625.87	1.8	0.29
3	338.6	1722.19	5.1	0.48
4	591.2	3290.67	5.6	0.48
5	682.5	3290.67	4.8	0.48
6	747.8	3290.67	4.4	0.47
7	747.8	3290.67	4.4	0.47
8	866.9	3384.04	3.9	0.46
9	866.9	3384.04	3.9	0.46
10	1018.4	3384.04	3.3	0.45
11	1018.4	3384.04	3.3	0.45
12	1195.6	3384.04	2.8	0.43
13	1195.6	3384.04	2.8	0.43
14	1286.9	3384.04	2.6	0.42
15	1286.9	3384.04	2.6	0.42
16	1286.9	3384.04	2.6	0.42
17	1286.9	3384.04	2.6	0.42
18	1286.9	3384.04	2.6	0.42
19	1286.9	3384.04	2.6	0.42
20	1286.9	3384.04	2.6	0.42
21	1286.9	3384.04	2.6	0.42
22	1286.9	3384.04	2.6	0.42
23	1286.9	3384.04	2.6	0.42
24	1286.9	3384.04	2.6	0.42
25	1286.9	3384.04	2.6	0.42
26	1286.9	3384.04	2.6	0.42
27	1286.9	3384.04	2.6	0.42
28	1286.9	3384.04	2.6	0.42
29	1286.9	3384.04	2.6	0.42
30	1286.9	3384.04	2.6	0.42

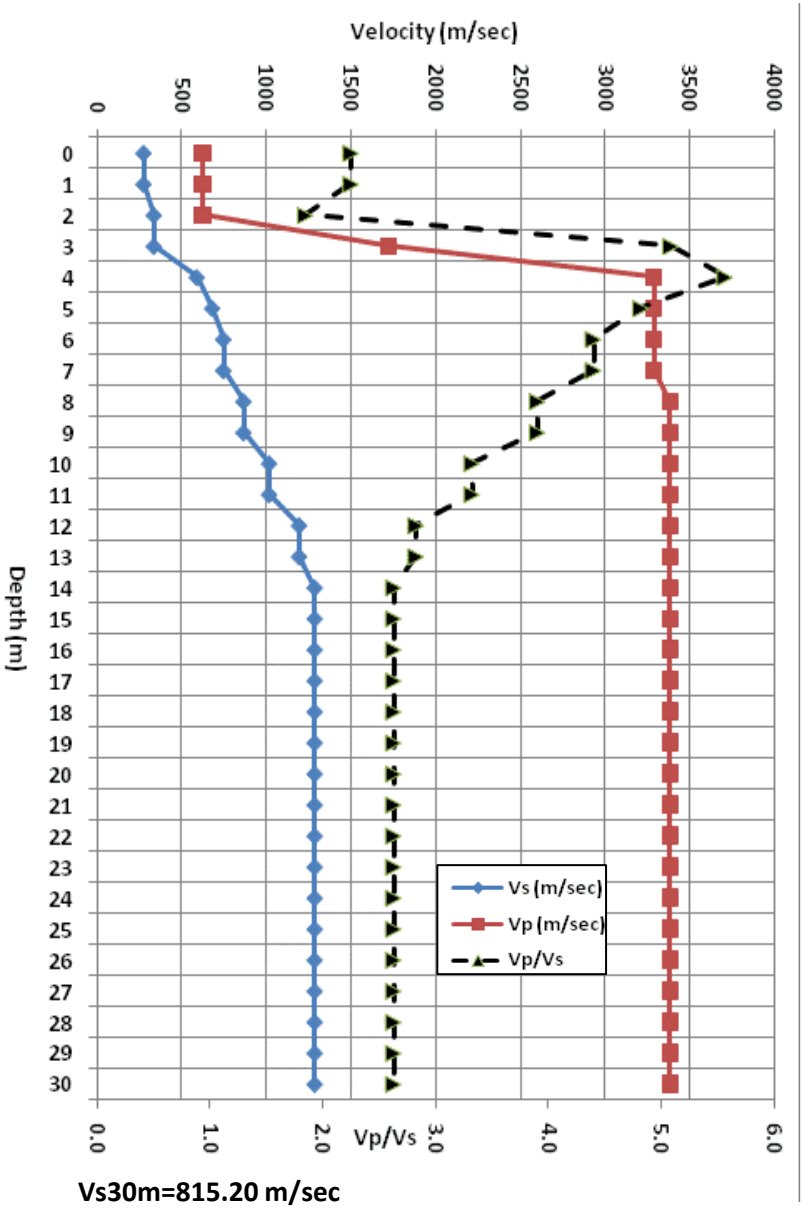

Figure A6. Vs, Vp, Vp/Vs and Poisson's Ratio profiles at GNW_2.

HART

Depth Interval (m)		Vs (m/sec)
0.0	1.6	94.92
1.6	3.5	90.62
3.5	5.7	100.63
5.7	8.1	117.16
8.1	10.7	128.00
10.7	13.6	132.33
13.6	16.8	138.02
16.8	20.2	146.58
20.2	23.9	154.44
23.9	27.8	162.98
27.8	30.0	170.91
30.0	32.0	170.91
32.0	36.4	176.67
36.4	41.1	176.52
41.1	46.0	177.63

Depth interval (m)		Vp (m/sec)
0.0	0.6	619.41
0.6	1.8	619.41
1.8	3.0	741.37
3.0	4.2	1089.22
4.2	7.1	1089.22
7.1	10.0	1089.22
10.0	12.9	1091.04
12.9	15.8	1160.44
15.8	18.7	1756.67
18.7	-	2767.54

Depth (m)	Vs (m/sec)	Vp (m/sec)	Vp/Vs	Poisson's Ratio
0	94.92	619.41	6.5	0.49
1	94.92	619.41	6.5	0.49
2	90.62	741.37	8.2	0.49
3	90.62	1089.22	12.0	0.50
4	100.63	1089.22	10.8	0.50
5	100.63	1089.22	10.8	0.50
6	117.16	1089.22	9.3	0.49
7	117.16	1089.22	9.3	0.49
8	128.00	1089.22	8.5	0.49
9	128.00	1089.22	8.5	0.49
10	128.00	1091.04	8.5	0.49
11	132.33	1091.04	8.2	0.49
12	132.33	1091.04	8.2	0.49
13	132.33	1160.44	8.8	0.49
14	138.02	1160.44	8.4	0.49
15	138.02	1160.44	8.4	0.49
16	138.02	1756.67	12.7	0.50
17	146.58	1756.67	12.0	0.50
18	146.58	2767.00	18.9	0.50
19	146.58	2767.00	18.9	0.50
20	154.44	2767.00	17.9	0.50
21	154.44	2767.00	17.9	0.50
22	154.44	2767.00	17.9	0.50
23	154.44	2767.00	17.9	0.50
24	162.98	2767.00	17.0	0.50
25	162.98	2767.00	17.0	0.50
26	162.98	2767.00	17.0	0.50
27	162.98	2767.00	17.0	0.50
28	170.91	2767.00	17.0	0.50
29	170.91	2767.00	17.0	0.50
30	170.91	2767.00	17.0	0.50

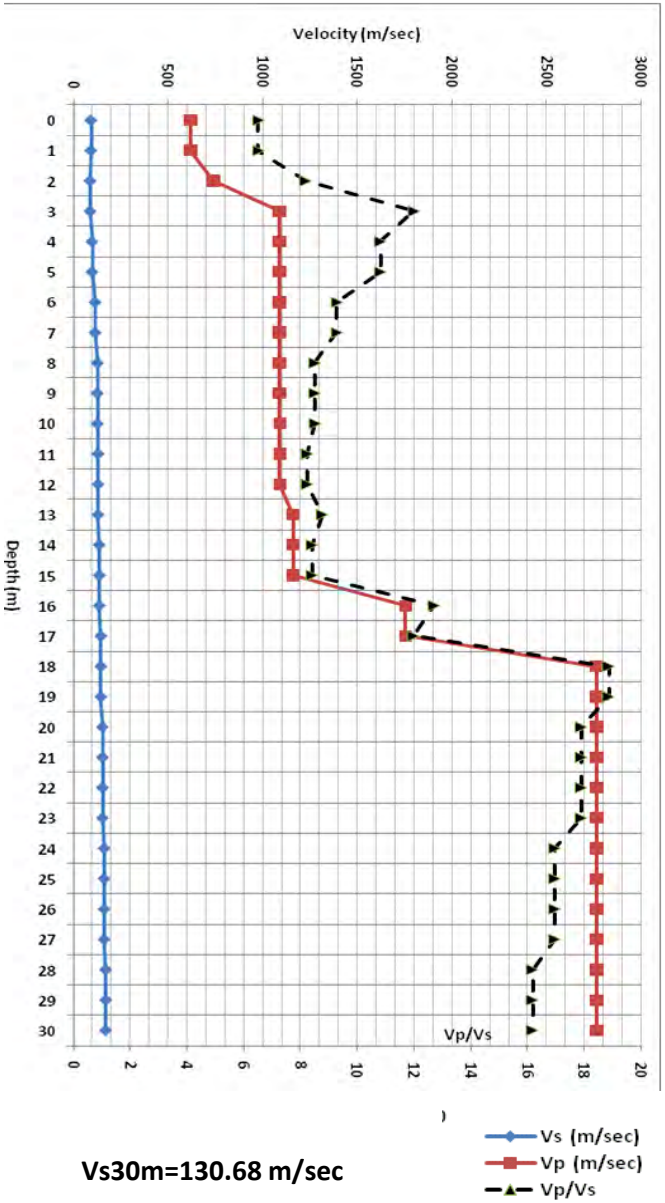

Vs30m=130.68 m/sec

Figure A7. Vs, Vp, Vp/Vs and Poisson's Ratio profiles at HART.

KCAM

Depth Interval (m)		Vs (m/sec)
0.0	1.3	115.12
1.3	2.8	157.96
2.8	4.4	163.58
4.4	6.1	160.98
6.1	8.0	166.26
8.0	10.1	173.50
10.1	12.3	181.55
12.3	14.6	190.56
14.6	17.1	198.97
17.1	19.7	205.18
19.7	22.5	205.18
22.5	25.4	205.18
25.4	28.5	205.18
28.5	31.7	205.18
31.7	35.1	205.18
35.1	38.6	204.29
38.6	42.1	203.09
42.1	46.1	203.43
46.1	50.0	205.18

Depth Interval (m)		Vp (m/sec) (Wong et al, 2003)
0.00	1.5	845
1.5	7.6	845
7.6	11.6	1541
11.6	15.2	1880
15.2	32.0	1420
32.0	40.5	1573
40.5	58.8	1306
58.8	61.9	1508
61.9	64.0	1899

Depth Interval (m)		Vs (m/sec)	Vp (m/sec) (Wong et al, 2003)	Vp/Vs	Poisson's Ratio
0.0	1.3	115.12	845.00	7.3	0.50
1.3	2.8	157.96	845.00	5.4	0.49
2.8	4.4	163.58	845.00	5.2	0.49
4.4	6.1	160.98	845.00	5.3	0.49
6.1	8.0	166.26	845.00	5.1	0.49
8.0	10.1	173.50	1541.00	8.9	0.50
10.1	12.3	181.55	1541.00	8.5	0.50
12.3	14.6	190.56	1880.00	9.9	0.50
14.6	17.1	198.97	1420.00	7.1	0.50
17.1	19.7	205.18	1420.00	6.9	0.49
19.7	22.5	205.18	1420.00	6.9	0.49
22.5	25.4	205.18	1420.00	6.9	0.49
25.4	28.5	205.18	1420.00	6.9	0.49
28.5	31.7	205.18	1420.00	6.9	0.49
31.7	35.1	205.18	1573.00	7.7	0.50
35.1	38.6	204.29	1573.00	7.7	0.50
38.6	42.3	203.09	1573.00	7.8	0.50
42.3	46.1	203.43	1306.00	6.4	0.49
46.1	50.0	205.18	1306.00	6.4	0.49

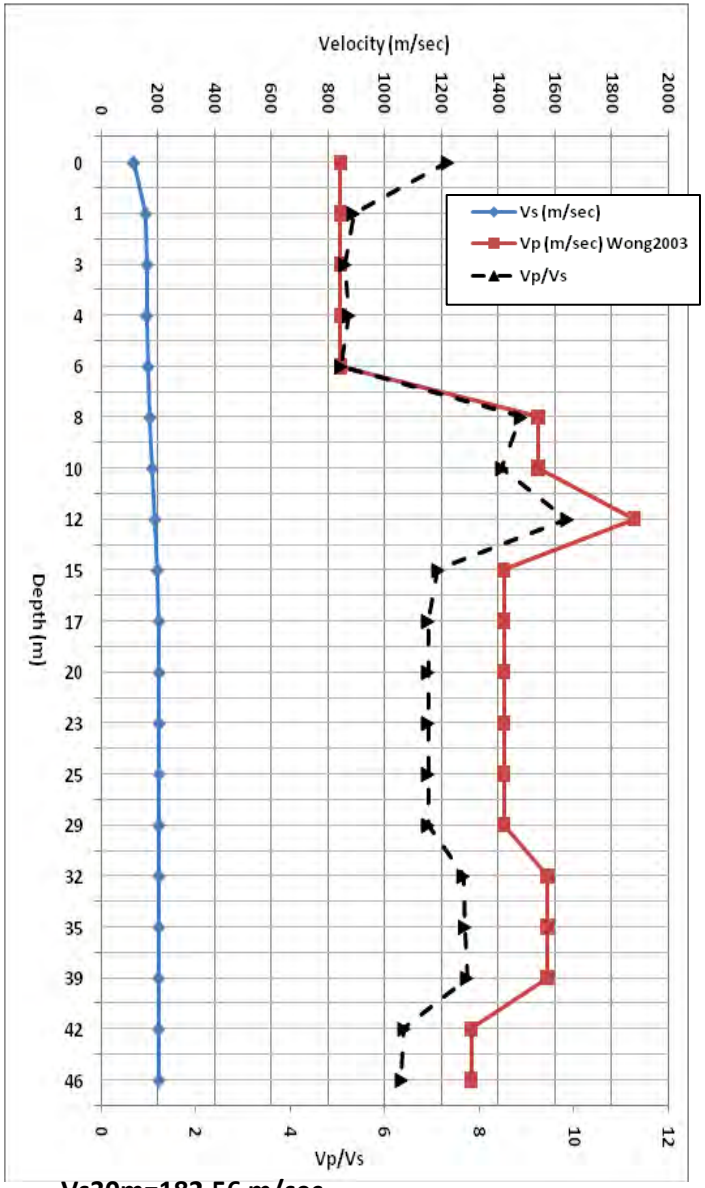

Vs30m=182.56 m/sec

Figure A8. Vs, Vp, Vp/Vs and Poisson's Ratio profiles at KCAM.

KNEL

Depth Interval (m)		Vs (m/sec)
0.0	1.1	166.78
1.1	2.3	148.10
2.3	3.7	124.58
3.7	5.3	144.70
5.3	7.0	145.69
7.0	8.9	153.90
8.9	11.0	167.41
11.0	13.2	182.36
13.2	15.6	195.20
15.6	18.1	207.30
18.1	20.9	218.90
20.9	23.7	220.43
23.7	26.8	220.43
26.8	30.0	220.43

Depth Interval (m)		Vp (m/sec)
0.0	0.9	587.01
0.9	2.8	593.75
2.8	4.7	596.41
4.7	6.6	599.77
6.6	11.1	1246.57
11.1	15.6	1573.83
15.6	20.1	1964.03
20.1	24.6	2686.81
24.6	29.1	3454.50
29.1	-	3454.50

Depth (m)	Vs (m/sec)	Vp (m/sec)	Vp/Vs	Poisson's Ratio
0	166.78	587.01	3.5	0.46
1	148.10	593.75	4.0	0.47
2	124.58	593.75	4.8	0.48
3	124.58	596.41	4.8	0.48
4	144.70	596.41	4.1	0.47
5	145.69	599.77	4.1	0.47
6	145.69	599.77	4.1	0.47
7	153.90	1246.57	8.1	0.49
8	153.90	1246.57	8.1	0.49
9	167.41	1246.57	7.5	0.49
10	167.41	1246.57	7.5	0.49
11	182.36	1573.83	8.6	0.49
12	182.36	1573.83	8.6	0.49
13	195.20	1573.83	8.1	0.49
14	195.20	1573.83	8.1	0.49
15	195.20	1573.83	8.1	0.49
16	207.30	1964.03	9.5	0.49
17	207.30	1964.03	9.5	0.49
18	218.90	1964.03	8.5	0.49
19	218.90	1964.03	8.5	0.49
20	218.90	2686.81	12.3	0.50
21	220.43	2686.81	12.2	0.50
22	220.43	2686.81	12.2	0.50
23	220.43	2686.81	12.2	0.50
24	220.43	2686.81	12.2	0.50
25	220.43	3454.50	15.7	0.50
26	220.43	3454.50	15.7	0.50
27	220.43	3454.50	15.7	0.50
28	220.43	3454.50	15.7	0.50
29	220.43	3454.50	15.7	0.50
30	220.43	3454.50	15.7	0.50

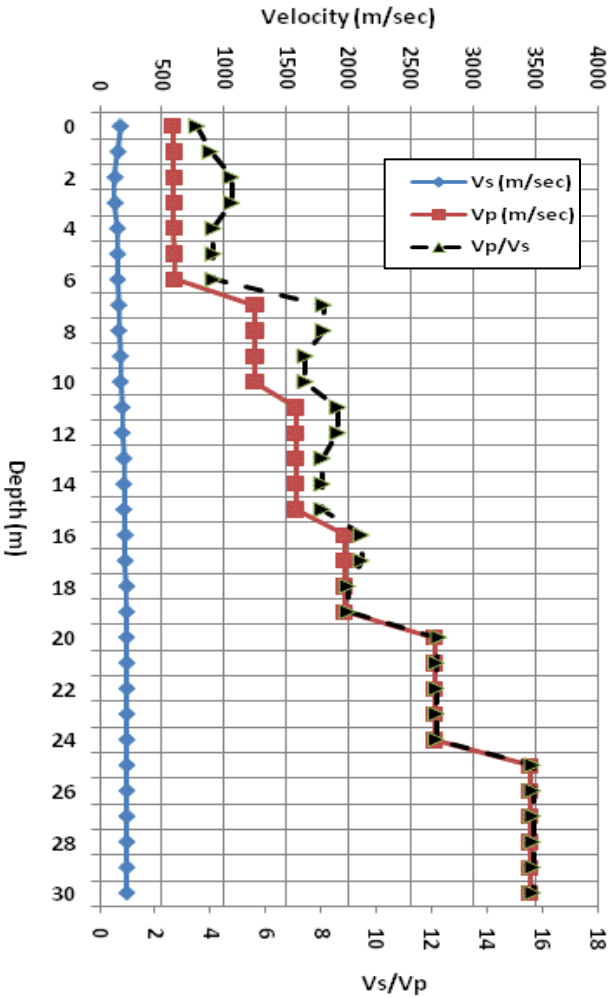

Vs30m=182.88 m/sec

Figure A9. Vs, Vp, Vp/Vs and Poisson's Ratio profiles at KNEL.

KNJH

Depth Interval (m)		Vs (m/sec)
0.0	1.0	118.77
1.0	2.2	105.59
2.2	3.4	94.36
3.4	4.7	103.20
4.7	6.1	128.40
6.1	7.6	144.60
7.6	9.2	153.16
9.2	10.9	173.14
10.9	12.6	191.07
12.6	14.5	208.17
14.5	16.4	226.01
16.4	18.5	243.06
18.5	20.6	259.45
20.6	22.8	271.59
22.8	25.1	279.75
25.1	27.5	289.82
27.5	30.0	302.88
30.0	32.6	319.68
32.6	35.3	340.54
35.3	38.0	365.46
38.0	40.9	394.06
40.9	43.8	403.86
43.8	46.9	438.06
46.9	50.0	473.32
50.0	0.0	473.32

Depth Interval (m)		Vp (m/sec)
0.0	0.9	457.59
0.9	2.8	462.36
2.8	4.7	470.92
4.7	6.6	471.44
6.6	11.1	1378.06
11.1	15.6	1657.90
15.6	20.1	1818.38
20.1	24.6	1819.38
24.6	29.1	1820.38
29.1	0.0	1821.38

Depth (m)	Vs (m/sec)	Vp (m/sec)	Vp/Vs	Poisson's Ratio
0	118.77	457.59	3.9	0.46
1	105.59	462.36	4.4	0.47
2	94.36	462.36	4.9	0.48
3	103.20	470.92	4.6	0.47
4	128.40	470.92	3.7	0.46
5	128.40	471.44	3.7	0.46
6	144.60	471.44	3.3	0.45
7	144.60	1378.06	9.5	0.49
8	153.16	1378.06	9.0	0.49
9	173.14	1378.06	8.0	0.49
10	173.14	1378.06	8.0	0.49
11	191.07	1657.90	8.7	0.49
12	191.07	1657.90	8.7	0.49
13	208.17	1657.90	8.0	0.49
14	208.17	1657.90	8.0	0.49
15	226.01	1657.90	7.3	0.49
16	243.06	1818.38	7.5	0.49
17	243.06	1818.38	7.5	0.49
18	243.06	1818.38	7.5	0.49
19	259.45	1818.38	7.0	0.49
20	259.45	1818.38	7.0	0.49
21	271.59	1818.38	6.7	0.49
22	271.59	1818.38	6.7	0.49
23	279.75	1818.38	6.5	0.49
24	279.75	1818.38	6.5	0.49
25	289.82	1818.38	6.3	0.49
26	289.82	1818.38	6.3	0.49
27	289.82	1818.38	6.3	0.49
28	302.88	1818.38	6.0	0.49
29	302.88	1818.38	6.0	0.49
30	319.68	1818.38	5.7	0.48

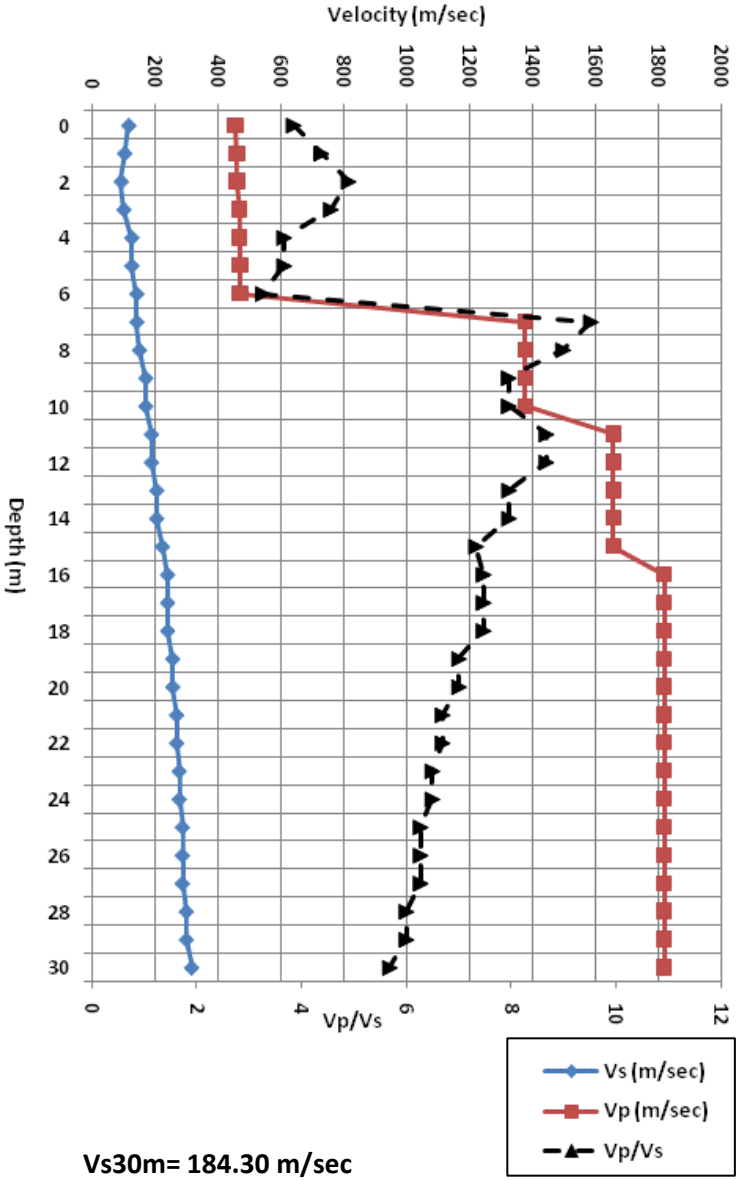

Vs30m= 184.30 m/sec

Figure A10. Vs, Vp, Vp/Vs and Poisson's Ratio profiles at KNJH.

LON

Depth Interval (m)		Vs (m/sec)
0.0	1.1	266.60
1.1	2.3	248.45
2.3	3.7	285.62
3.7	5.3	458.41
5.3	7.0	511.80
7.0	8.9	571.09
8.9	11.0	639.48
11.0	13.2	720.03
13.2	15.6	830.94
15.6	18.1	983.30
18.1	20.9	1122.80
20.9	23.7	1258.97
23.7	26.8	1296.82
26.8	30.0	1296.82

Depth Interval (m)		Vp (m/sec)
0.0	0.8	576.61
0.8	2.5	578.26
2.5	4.2	584.29
4.2	5.8	586.89
5.8	7.5	587.69
7.5	9.2	652.12
9.2	12.9	2122.43
12.9	16.7	2122.43
16.7	20.4	2731.07
20.4	24.2	3503.76
24.2	27.9	3666.48
27.9	31.7	3666.48

Depth (m)	Vs (m/sec)	Vp (m/sec)	Vp/Vs	Poisson's Ratio
0	266.60	576.61	2.2	0.36
1	248.45	578.26	2.3	0.39
2	285.62	584.29	2.0	0.34
3	458.41	1079.51	2.4	0.39
4	511.80	1205.22	2.4	0.39
5	511.80	1205.22	2.4	0.39
6	571.09	1344.85	2.4	0.39
7	571.09	1344.85	2.4	0.39
8	639.48	2122.43	3.3	0.45
9	639.48	2122.43	3.3	0.45
10	720.03	2122.43	2.9	0.43
11	720.03	2122.43	2.9	0.43
12	830.94	2122.43	2.6	0.41
13	830.94	2122.43	2.6	0.41
14	830.94	2122.43	2.6	0.41
15	983.30	2122.43	2.2	0.36
16	983.30	2731.07	2.8	0.43
17	1122.80	2731.07	2.4	0.40
18	1122.80	2731.07	2.4	0.40
19	1122.80	3503.76	3.1	0.44
20	1258.97	3503.76	2.8	0.43
21	1258.97	3503.76	2.8	0.43
22	1258.97	3503.76	2.8	0.43
23	1296.82	3666.48	2.8	0.43
24	1296.82	3666.48	2.8	0.43
25	1296.82	3666.48	2.8	0.43
26	1296.82	3666.48	2.8	0.43
27	1296.82	3666.48	2.8	0.43
28	1296.82	3666.48	2.8	0.43
29	1296.82	3666.48	2.8	0.43
30	1296.82	3666.48	2.8	0.43

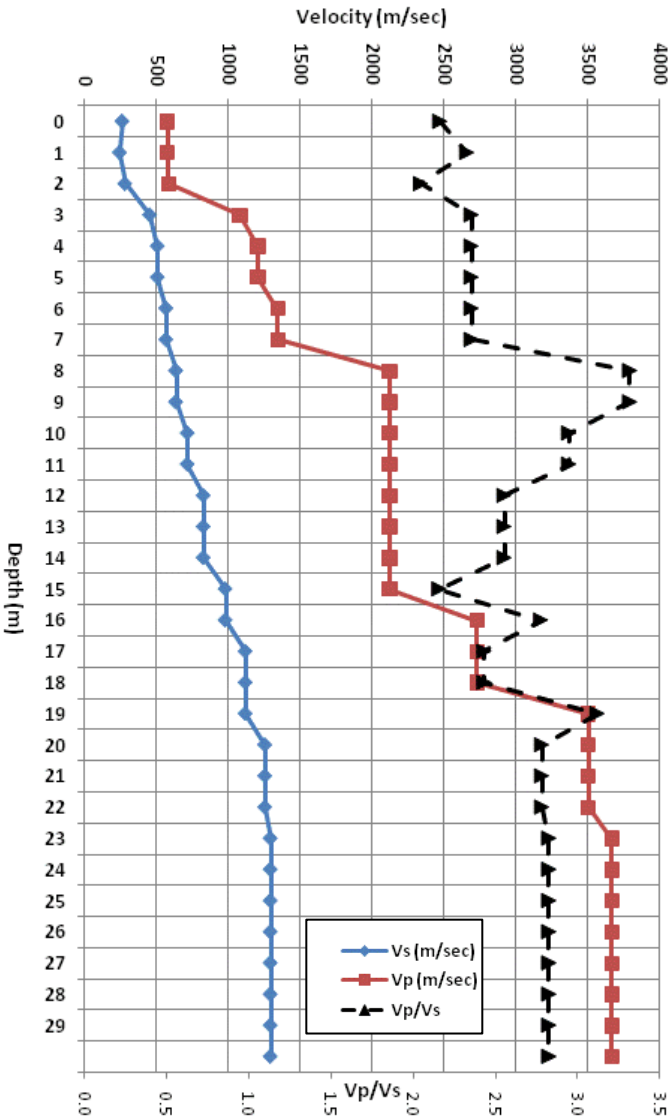

Vs30m=661.55 m/sec

Figure A11. Vs, Vp, Vp/Vs and Poisson's Ratio profiles at LON.

LTY

Depth Interval (m)		Vs (m/sec)
0.0	1.1	629.98
1.1	2.3	624.21
2.3	3.7	611.90
3.7	5.3	605.72
5.3	7.0	648.26
7.0	8.9	725.81
8.9	11.0	802.95
11.0	13.2	897.15
13.2	15.6	905.45
15.6	18.1	1018.78
18.1	20.9	1028.15
20.9	23.7	1161.40
23.7	26.8	1184.31
26.8	30.0	1201.42
30.0	-	1201.42

Depth Interval (m)		Vp (m/sec)
0.0	1.6	396.46
1.6	4.7	1349.46
4.7	7.8	1645.40
7.8	10.9	2042.50
10.9	18.4	2390.27
18.4	25.9	2390.41
25.9	33.4	2390.41
33.4	40.9	2390.41
40.9	48.4	2390.41
48.4	-	2390.41

Depth (m)	Vs (m/sec)	Vp (m/sec)	Vp/Vs	Poisson's Ratio
0.0	629.98	1349.46	2.1	0.36
1.0	624.21	1349.46	2.2	0.36
2.0	611.90	1349.46	2.2	0.37
3.0	611.90	1349.46	2.2	0.37
4.0	605.72	1349.46	2.2	0.37
5.0	648.26	1645.40	2.5	0.41
6.0	648.26	1645.40	2.5	0.41
7.0	725.81	1645.40	2.3	0.38
8.0	725.81	2042.50	2.8	0.43
9.0	802.95	2042.50	2.5	0.41
10.0	802.95	2042.50	2.5	0.41
11.0	897.15	2390.27	2.7	0.42
12.0	897.15	2390.27	2.7	0.42
13.0	905.45	2390.27	2.6	0.42
14.0	905.45	2390.27	2.6	0.42
15.0	905.45	2390.27	2.6	0.42
16.0	1018.78	2390.27	2.4	0.39
17.0	1018.78	2390.27	2.4	0.39
18.0	1028.15	2390.41	2.3	0.39
19.0	1028.15	2390.41	2.3	0.39
20.0	1028.15	2390.41	2.3	0.39
21.0	1161.40	2390.41	2.1	0.35
22.0	1161.40	2390.41	2.1	0.35
23.0	1161.40	2390.41	2.1	0.35
24.0	1184.31	2390.41	2.0	0.34
25.0	1184.31	2390.41	2.0	0.34
26.0	1184.31	2390.41	2.0	0.34
27.0	1201.42	2390.41	2.0	0.33
28.0	1201.42	2390.41	2.0	0.33
29.0	1201.42	2390.41	2.0	0.33
30.0	1201.42	2390.41	2.0	0.33

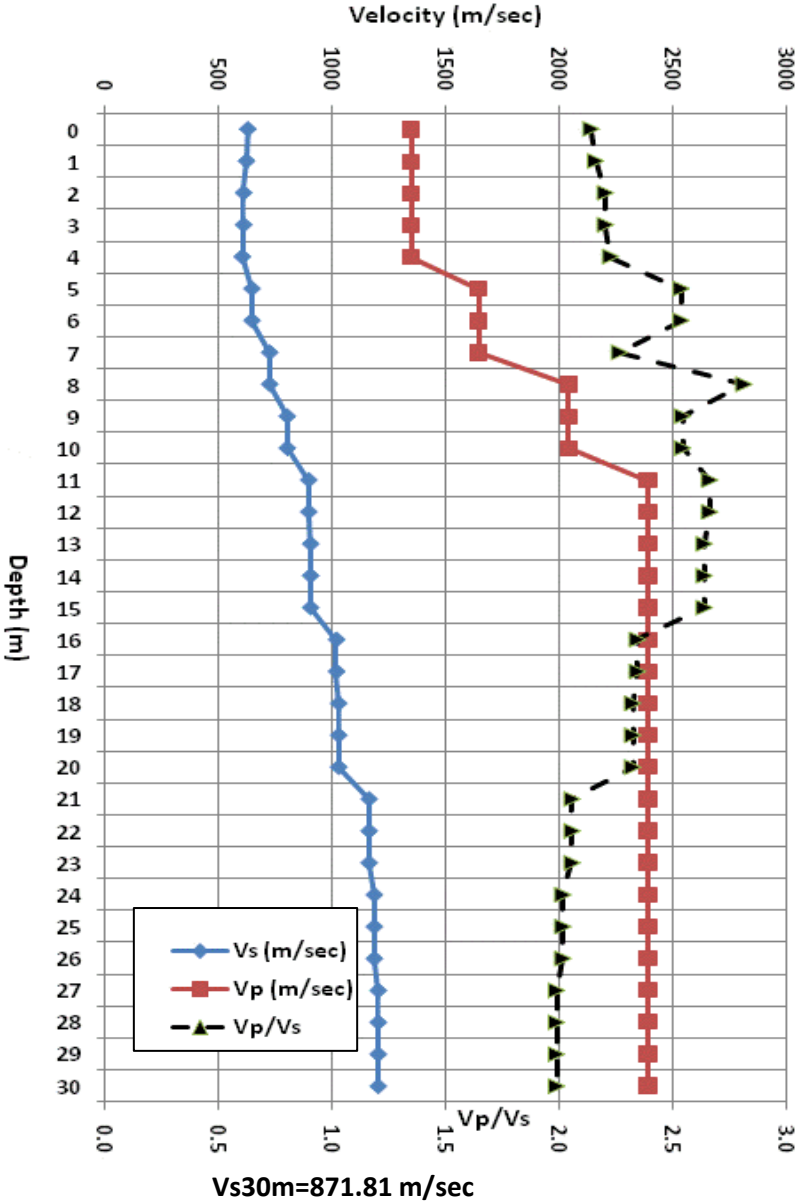

Figure A12. Vs, Vp, Vp/Vs and Poisson's Ratio profiles at LTY.

LYCH

Depth Interval (m)		Vs (m/sec)
0.0	1.1	563.91
1.1	2.3	570.22
2.3	3.7	567.86
3.7	5.3	528.98
5.3	7.0	476.52
7.0	8.9	476.52
8.9	11.0	517.68
11.0	13.2	598.93
13.2	15.6	682.97
15.6	30.0	740.15

Depth Interval (m)		Vp (m/sec)
0.0	0.6	351.04
0.6	1.9	343.63
1.9	3.1	1141.27
3.1	4.4	1708.93
4.4	5.6	1880.44
5.6	6.9	1936.55
6.9	9.7	1957.65
9.7	12.5	2302.93
12.5	15.3	2585.78
15.3	18.1	2735.73
18.1	20.9	2735.73
20.9	23.8	2735.73
23.8	26.6	2735.73
26.6	29.4	2735.73

Depth (m)	Vs (m/sec)	Vp (m/sec)	Vp/Vs	Poisson's Ratio
0	563.91	1119.50	2.0	0.33
1	570.22	1132.02	2.0	0.33
2	567.86	1141.27	2.0	0.34
3	567.86	1708.93	3.0	0.44
4	528.98	1880.44	3.6	0.46
5	476.52	1880.44	4.0	0.47
6	476.52	1936.55	4.1	0.47
7	476.52	1957.65	4.1	0.47
8	476.52	1957.65	4.1	0.47
9	517.68	1957.65	3.8	0.46
10	517.68	2302.93	4.5	0.47
11	598.93	2302.93	3.9	0.46
12	598.93	2302.93	3.9	0.46
13	682.97	2585.78	3.8	0.46
14	682.97	2585.78	3.8	0.46
15	682.97	2735.73	4.0	0.47
16	740.15	2735.73	3.7	0.46
17	740.15	2735.73	3.7	0.46
18	740.15	2735.73	3.7	0.46
19	740.15	2735.73	3.7	0.46
20	740.15	2735.73	3.7	0.46
21	740.15	2735.73	3.7	0.46
22	740.15	2735.73	3.7	0.46
23	740.15	2735.73	3.7	0.46
24	740.15	2735.73	3.7	0.46
25	740.15	2735.73	3.7	0.46
26	740.15	2735.73	3.7	0.46
27	740.15	2735.73	3.7	0.46
28	740.15	2735.73	3.7	0.46
29	740.15	2735.73	3.7	0.46
30	740.15	2735.73	3.7	0.46

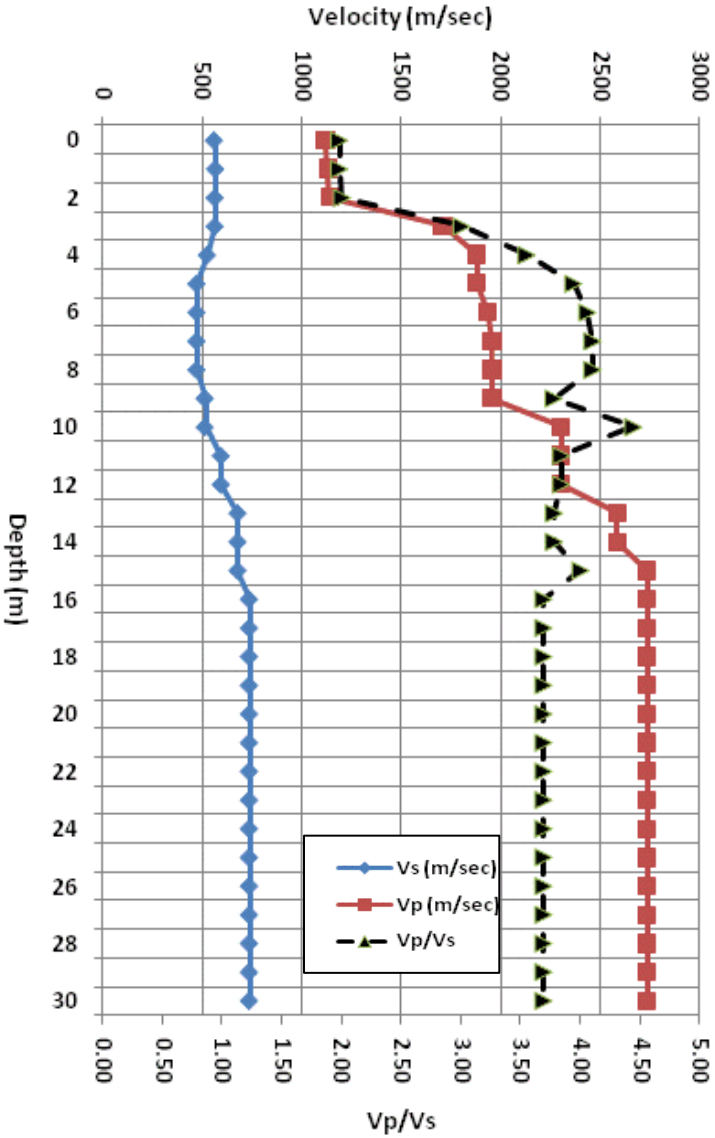

Vs30m= 627.78 m/sec

Figure A13. Vs, Vp, Vp/Vs and Poisson's Ratio profiles at LYCH.

PAYL

Depth interval (m)		Vs (m/sec)
0.0	1.1	107.74
1.1	2.3	104.28
2.3	3.7	102.32
3.7	5.3	119.28
5.3	7.0	134.18
7.0	8.9	152.05
8.9	11.0	166.18
11.0	13.2	177.99
13.2	15.6	191.04
15.6	18.1	196.85
18.1	20.9	201.04
20.9	23.7	204.67
23.7	26.8	207.59
26.8	30.0	209.93
30.0	-	211.91

Depth Interval (m)		Vp (m/sec)
0.0	0.9	382.93
0.9	2.8	427.82
2.8	4.7	471.92
4.7	6.6	1149.92
6.6	11.1	1239.43
11.1	15.6	1240.43
15.6	20.1	1243.78
20.1	24.6	1244.65
24.6	29.1	1245.53
29.1	-	1246.41

Depth (m)	Vs (m/sec)	Vp (m/sec)	Vp/Vs	Poisson's Ratio
0	107.74	382.93	3.6	0.46
1	104.28	427.82	4.1	0.47
2	102.32	427.82	4.2	0.47
3	102.32	471.92	4.6	0.48
4	119.28	471.92	4.0	0.47
5	134.18	1149.92	8.6	0.49
6	134.18	1149.92	8.6	0.49
7	152.05	1239.43	8.2	0.49
8	152.05	1239.43	8.2	0.49
9	166.18	1239.43	7.5	0.49
10	166.18	1239.43	7.5	0.49
11	177.99	1240.43	7.0	0.49
12	177.99	1240.43	7.0	0.49
13	191.04	1240.43	6.5	0.49
14	191.04	1240.43	6.5	0.49
15	191.04	1240.43	6.5	0.49
16	196.85	1243.78	6.3	0.49
17	196.85	1243.78	6.3	0.49
18	201.04	1243.78	6.2	0.49
19	201.04	1243.78	6.2	0.49
20	201.04	1244.65	6.2	0.49
21	204.67	1244.65	6.1	0.49
22	204.67	1244.65	6.1	0.49
23	204.67	1244.65	6.1	0.49
24	207.59	1244.65	6.0	0.49
25	207.59	1245.53	6.0	0.49
26	207.59	1245.53	6.0	0.49
27	209.93	1245.53	5.9	0.49
28	209.93	1245.53	5.9	0.49
29	209.93	1245.53	5.9	0.49
30	209.93	1246.41	5.9	0.49

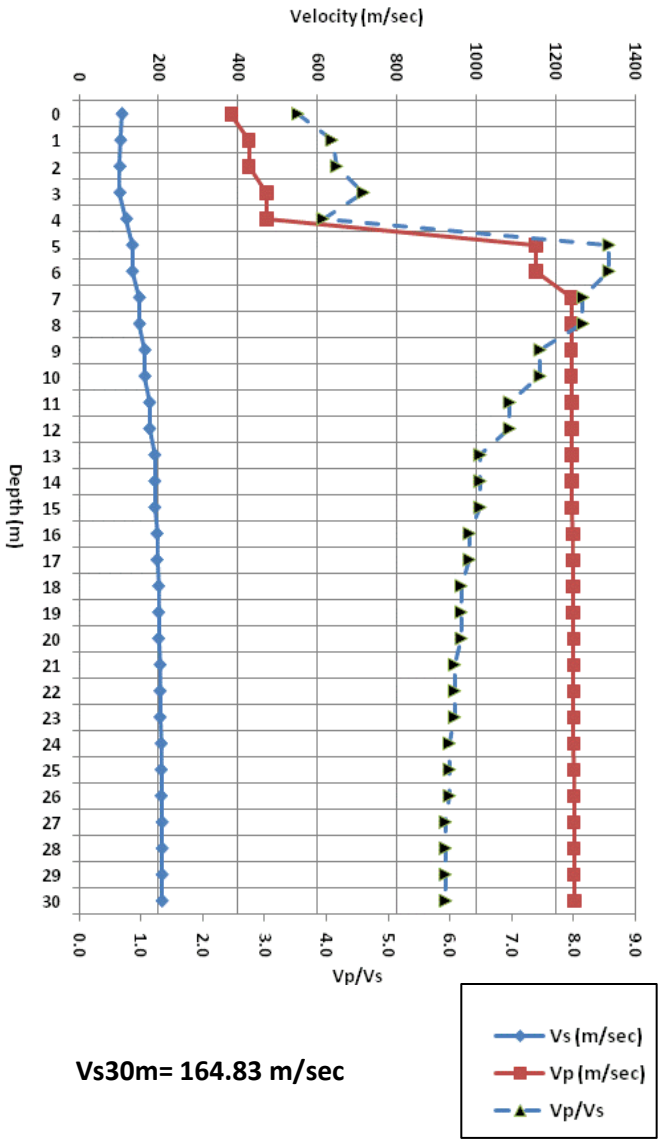

Vs30m= 164.83 m/sec

Figure A14. Vs, Vp, Vp/Vs and Poisson's Ratio profiles at PAYL.

SBES

Depth Interval (m)		Vs (m/sec)
0.0	1.1	300.16
1.1	2.2	215.45
2.2	3.5	291.44
3.5	4.9	383.00
4.9	6.4	493.80
6.4	8.1	566.77
8.1	9.8	611.74
9.8	11.7	679.62
11.7	13.7	758.85
13.7	15.8	830.69
15.8	18.0	889.10
18.0	20.4	922.68
20.4	22.8	955.71
22.8	30.0	958.22
30.0	-	

Depth Interval (m)		Vp (m/sec)
0.0	0.9	965.47
0.9	2.8	1034.78
2.8	4.7	1088.34
4.7	6.6	1133.87
6.6	11.1	2342.33
11.1	15.6	2355.82
15.6	20.1	2356.82
20.1	24.6	2357.82
24.6	29.1	2358.82
29.1	-	2359.82

Depth (m)	Vs (m/sec)	Vp (m/sec)	Vp/Vs	Poisson's Ratio
0	300.16	965.47	3.2	0.45
1	215.45	1034.78	4.8	0.48
2	291.44	1034.78	3.6	0.46
3	291.44	1088.34	3.7	0.46
4	383.00	1088.34	2.8	0.43
5	493.80	1133.87	2.3	0.38
6	566.77	1133.87	2.0	0.33
7	566.77	2342.33	4.1	0.47
8	611.74	2342.33	3.8	0.46
9	611.74	2342.33	3.8	0.46
10	679.62	2342.33	3.5	0.45
11	679.62	2355.82	3.5	0.45
12	758.85	2355.82	3.1	0.44
13	758.85	2355.82	3.1	0.44
14	830.69	2355.82	2.8	0.43
15	830.69	2355.82	2.8	0.43
16	889.10	2356.82	2.7	0.42
17	889.10	2357.82	2.7	0.42
18	922.68	2357.82	2.6	0.41
19	922.68	2357.82	2.6	0.41
20	922.68	2357.82	2.6	0.41
21	955.71	2357.82	2.5	0.40
22	955.71	2357.82	2.5	0.40
23	958.22	2357.82	2.5	0.40
24	958.22	2357.82	2.5	0.40
25	958.22	2357.82	2.5	0.40
26	958.22	2357.82	2.5	0.40
27	958.22	2357.82	2.5	0.40
28	958.22	2357.82	2.5	0.40
29	958.22	2357.82	2.5	0.40
30	958.22	2357.82	2.5	0.40

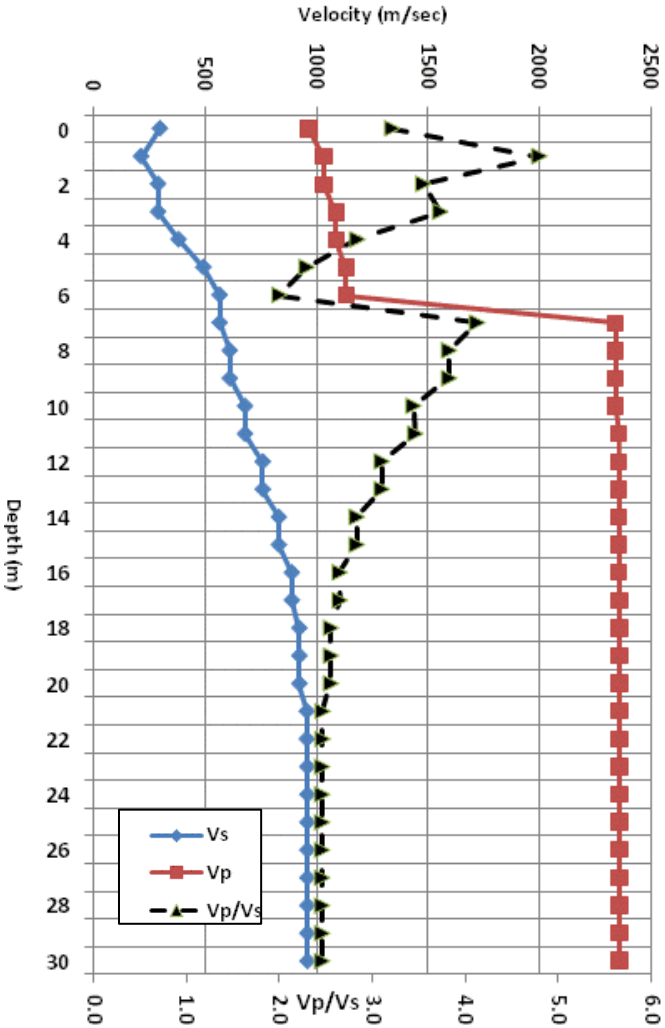

Vs30m= 613.88 m/sec

Figure A15. Vs, Vp, Vp/Vs and Poisson's Ratio profiles at SBES.

SFER

Depth Interval (m)		Vs (m/sec)
0.0	1.1	609.32
1.1	2.2	605.74
2.2	3.5	607.65
3.5	4.9	612.09
4.9	6.4	642.21
6.4	8.1	668.86
8.1	9.8	664.61
9.8	11.7	598.28
11.7	13.7	561.68
13.7	15.8	548.10
15.8	18.0	547.98
18.0	20.4	570.19
20.4	22.8	613.23
22.8	25.4	621.91
25.4	28.1	684.67
28.1	30.9	746.58
30.9	33.8	766.38
33.8	36.8	779.49
36.8	40.0	779.49
40.0	-	779.49

Depth Interval (m)		Vp (m/sec)
0.0	0.9	558.15
0.9	2.8	577.19
2.8	4.7	1437.44
4.7	6.6	1768.29
6.6	11.1	1768.29
11.1	15.6	1976.21
15.6	20.1	3344.13
20.1	24.6	4546.92
24.6	29.1	5062.07
29.1	-	5388.11

** Vp is calculated from Vs based on this assumed Poison's Ratio value.*

Depth (m)	Vs (m/sec)	Vp (m/sec)	Vp/Vs	Poisson's Ratio
0	609.32	1492.52	2.5	0.40*
1	605.74	1483.75	2.5	0.40*
2	607.65	1488.42	2.5	0.40*
3	607.65	1437.44	2.4	0.39
4	612.09	1437.44	2.4	0.39
5	642.21	1768.29	2.8	0.42
6	668.86	1768.29	2.6	0.42
7	668.86	1768.29	2.6	0.42
8	664.61	1768.29	2.7	0.42
9	664.61	1768.29	2.7	0.42
10	598.28	1768.29	3.0	0.44
11	598.28	1976.21	3.3	0.45
12	561.68	1976.21	3.5	0.46
13	561.68	1976.21	3.5	0.46
14	548.10	1976.21	3.6	0.46
15	548.10	1976.21	3.6	0.46
16	547.98	3344.13	6.1	0.49
17	547.98	3344.13	6.1	0.49
18	570.19	3344.13	5.9	0.49
19	570.19	3344.13	5.9	0.49
20	613.23	4546.92	7.4	0.49
21	613.23	4546.92	7.4	0.49
22	613.23	4546.92	7.4	0.49
23	621.91	4546.92	7.3	0.49
24	621.91	4546.92	7.3	0.49
25	684.67	4546.92	6.6	0.49
26	684.67	5062.07	7.4	0.49
27	684.67	5062.07	7.4	0.49
28	746.58	5062.07	6.8	0.49
29	746.58	5388.11	7.2	0.49
30	746.58	5388.11	7.2	0.49

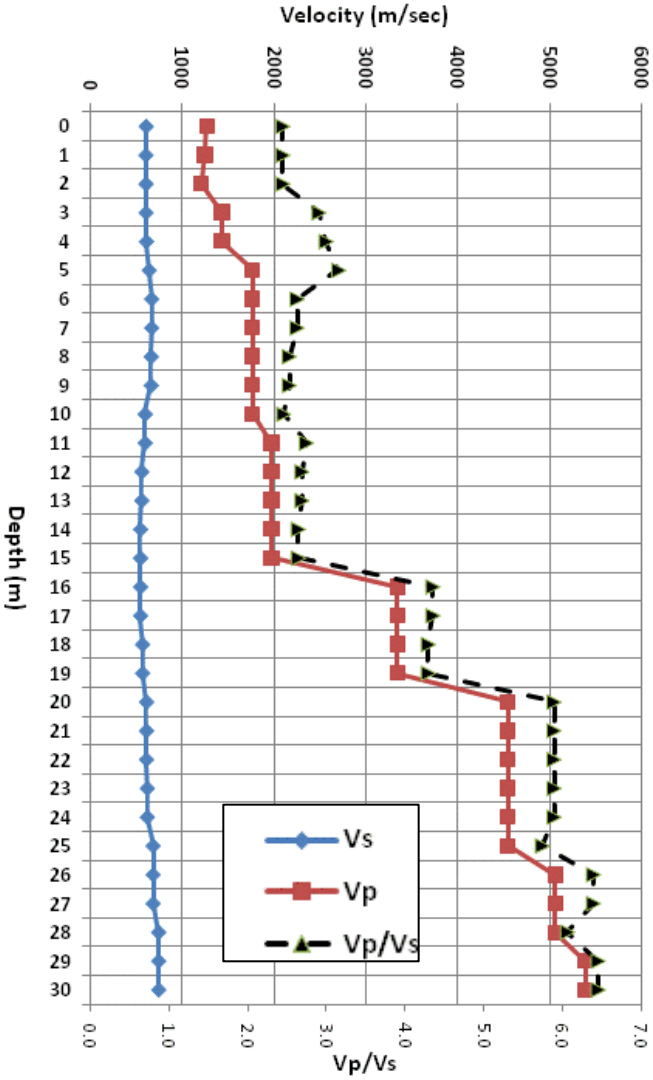

Vs30m= 614.16 m/sec

Figure A16. Vs, Vp, Vp/Vs and Poisson's Ratio profiles at SFES.

SMNR

Depth Interval (m)		Vs (m/sec)
0.0	1.8	85.00
1.8	3.8	78.20
3.8	6.2	104.59
6.2	8.8	135.26
8.8	11.7	161.09
11.7	14.8	184.06
14.8	18.3	206.41
18.3	22.0	232.61
22.0	26.0	258.62
26.0	30.2	280.45
30.2	34.8	287.72
34.8	39.6	290.42

Depth Interval (m)		Vp (m/sec)
0.0	0.9	514.14
0.9	2.8	514.67
2.8	4.7	515.28
4.7	6.6	515.33
6.6	11.1	985.12
11.1	15.6	1981.28
15.6	20.1	1988.24
20.1	24.6	2005.83
24.6	29.1	2006.83
29.1	-	2007.83

Depth (m)	Vs (m/sec)	Vp (m/sec)	Vp/Vs	Poisson's Ratio
0	85.00	514.14	6.0	0.49
1	85.00	514.67	6.1	0.49
2	78.20	514.67	6.6	0.49
3	78.20	515.28	6.6	0.49
4	104.59	515.28	4.9	0.48
5	104.59	515.33	4.9	0.48
6	135.26	515.33	3.8	0.46
7	135.26	985.12	7.3	0.49
8	135.26	985.12	7.3	0.49
9	161.09	985.12	6.1	0.49
10	161.09	985.12	6.1	0.49
11	161.09	1981.28	12.3	0.50
12	184.06	1981.28	10.8	0.50
13	184.06	1981.28	10.8	0.50
14	184.06	1981.28	10.8	0.50
15	206.41	1981.28	9.6	0.49
16	206.41	1988.24	9.6	0.49
17	206.41	1988.24	9.6	0.49
18	232.61	1988.24	8.5	0.49
19	232.61	1988.24	8.5	0.49
20	232.61	2005.83	8.6	0.49
21	232.61	2005.83	8.6	0.49
22	258.62	2005.83	7.8	0.49
23	258.62	2005.83	7.8	0.49
24	258.62	2005.83	7.8	0.49
25	258.62	2005.83	7.8	0.49
26	280.45	2005.83	7.2	0.49
27	280.45	2005.83	7.2	0.49
28	280.45	2005.83	7.2	0.49
29	280.45	2005.83	7.2	0.49
30	287.72	2005.83	7.0	0.49

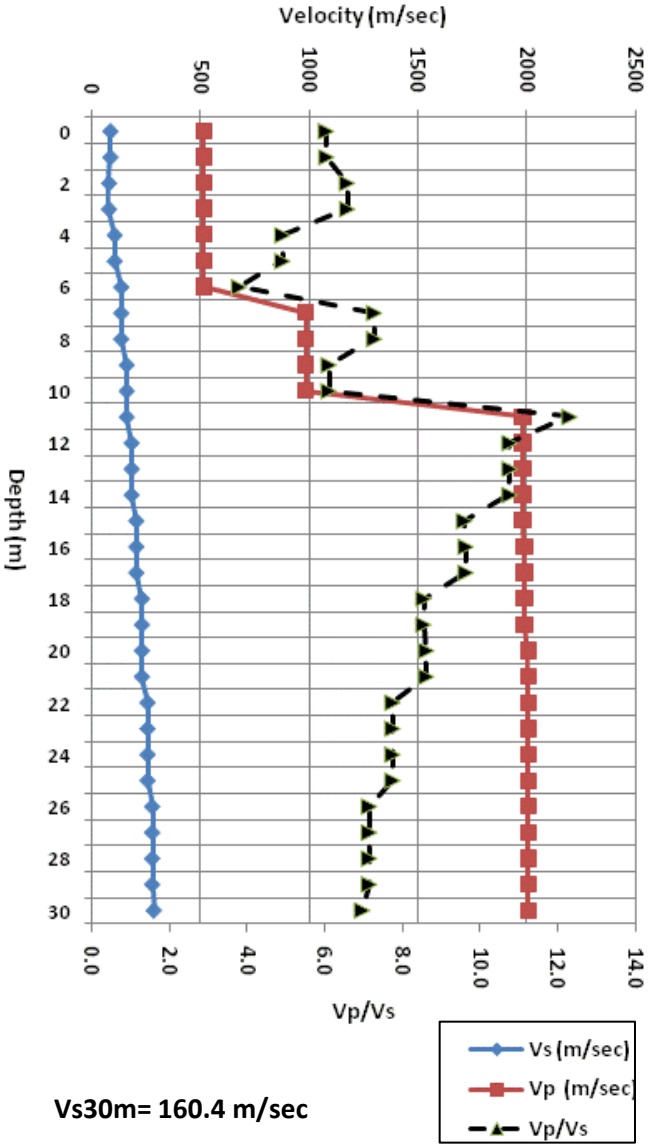

Vs30m= 160.4 m/sec

Figure A17. Vs, Vp, Vp/Vs and Poisson's Ratio profiles at SMNR.

SVTR

Depth Interval (m)		Vs (m/sec)
0.00	1.05	253.54
1.05	2.22	252.97
2.22	3.51	257.09
3.51	4.91	273.44
4.91	6.43	279.37
6.43	8.07	279.32
8.07	9.82	278.55
9.82	11.70	276.99
11.70	13.68	276.35
13.68	15.79	277.34
15.79	18.01	278.01
18.01	20.35	280.08
20.35	22.81	283.16
22.81	25.38	286.70
25.38	28.07	290.15
28.07	30.88	292.91
30.88	33.80	294.45
33.80	36.84	294.28
36.84	40.00	291.92
40.00	-	294.45

Depth Interval (m)		Vp (m/sec)
0.0	0.7	353.34
0.7	2.2	349.20
2.2	3.6	913.02
3.6	5.0	1262.23
5.0	8.5	1564.20
8.5	11.9	2258.58
11.9	15.4	2787.87
15.4	18.8	2988.24
18.8	22.3	2991.61
22.3	30.0	2991.87

Depth (m)	Vs (m/sec)	Vp (m/sec)	Vp/Vs	Poisson's Ratio
0	253.54	840.91	3.3	0.45
1	252.97	839.01	3.3	0.45
2	257.09	913.02	3.6	0.46
3	273.44	913.02	3.3	0.45
4	273.44	1262.23	4.6	0.48
5	279.37	1564.20	5.6	0.48
6	279.32	1564.20	5.6	0.48
7	279.32	1564.20	5.6	0.48
8	278.55	1564.20	5.6	0.48
9	278.55	2258.58	8.1	0.49
10	276.99	2258.58	8.2	0.49
11	276.99	2258.58	8.2	0.49
12	276.35	2787.87	10.1	0.50
13	276.35	2787.87	10.1	0.50
14	277.34	2787.87	10.1	0.50
15	277.34	2988.24	10.8	0.50
16	278.01	2988.24	10.8	0.50
17	278.01	2988.24	10.8	0.50
18	280.08	2988.24	10.7	0.50
19	280.08	2991.61	10.7	0.50
20	283.16	2991.61	10.6	0.50
21	283.16	2991.61	10.6	0.50
22	283.16	2991.87	10.6	0.50
23	286.70	2991.87	10.4	0.50
24	286.70	2991.87	10.4	0.50
25	290.15	2991.87	10.3	0.50
26	290.15	2991.87	10.3	0.50
27	290.15	2991.87	10.3	0.50
28	292.91	2991.87	10.2	0.50
29	292.91	2991.87	10.2	0.50
30	292.91	2991.87	10.2	0.50

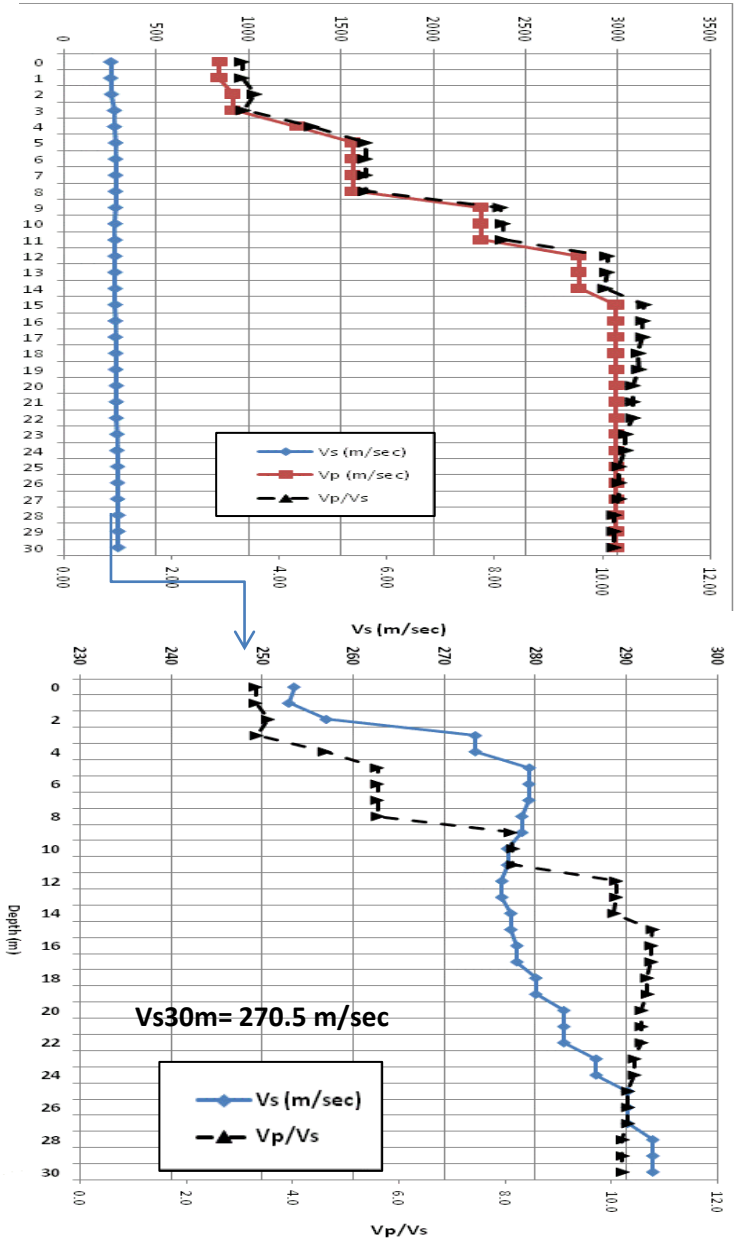

Figure A18. Vs, Vp, Vp/Vs and Poisson's Ratio profiles at SVTR.

UWFH

Depth Interval (m)		Vs (m/sec)
0.0	2.9	230.66
2.9	5.7	353.08
5.7	8.6	473.55
8.6	11.4	584.99
11.4	14.3	618.02
14.3	17.1	631.90
17.1	20.0	633.13
20.0	22.9	626.74
22.9	25.7	617.25
25.7	28.6	607.62
28.6	31.4	599.30
31.4	34.3	592.79
34.3	37.1	588.00
37.1	37.1	584.63
37.1	-	633.13

Depth Interval (m)		Vp (m/sec)
0.0	0.9	1380.86
0.9	2.8	1398.76
2.8	4.7	1455.70
4.7	6.6	1455.70
6.6	11.1	1455.70
11.1	15.6	1482.52
15.6	20.1	1504.07
20.1	24.6	1557.91
24.6	29.1	1616.16
29.1	0.0	1689.15

Depth (m)	Vs (m/sec)	Vp (m/sec)	Vp/Vs	Poisson's Ratio
0	230.66	1380.86	5.99	0.49
1	230.66	1398.76	6.06	0.49
2	230.66	1398.76	6.06	0.49
3	353.08	1455.70	4.12	0.47
4	353.08	1455.70	4.12	0.47
5	353.08	1455.70	4.12	0.47
6	473.55	1455.70	3.07	0.44
7	473.55	1455.70	3.07	0.44
8	473.55	1455.70	3.07	0.44
9	584.99	1455.70	2.49	0.40
10	584.99	1455.70	2.49	0.40
11	618.02	1482.52	2.40	0.39
12	618.02	1482.52	2.40	0.39
13	618.02	1482.52	2.40	0.39
14	631.90	1482.52	2.35	0.39
15	631.90	1482.52	2.35	0.39
16	631.90	1504.07	2.38	0.39
17	633.13	1504.07	2.38	0.39
18	633.13	1504.07	2.38	0.39
19	633.13	1504.07	2.38	0.39
20	626.74	1557.91	2.49	0.40
21	626.74	1557.91	2.49	0.40
22	626.74	1557.91	2.49	0.40
23	617.25	1557.91	2.52	0.41
24	617.25	1557.91	2.52	0.41
25	607.62	1616.16	2.66	0.42
26	607.62	1616.16	2.66	0.42
27	607.62	1616.16	2.66	0.42
28	607.62	1616.16	2.66	0.42
29	599.30	1689.15	2.82	0.43
30	599.30	1689.15	2.82	0.43

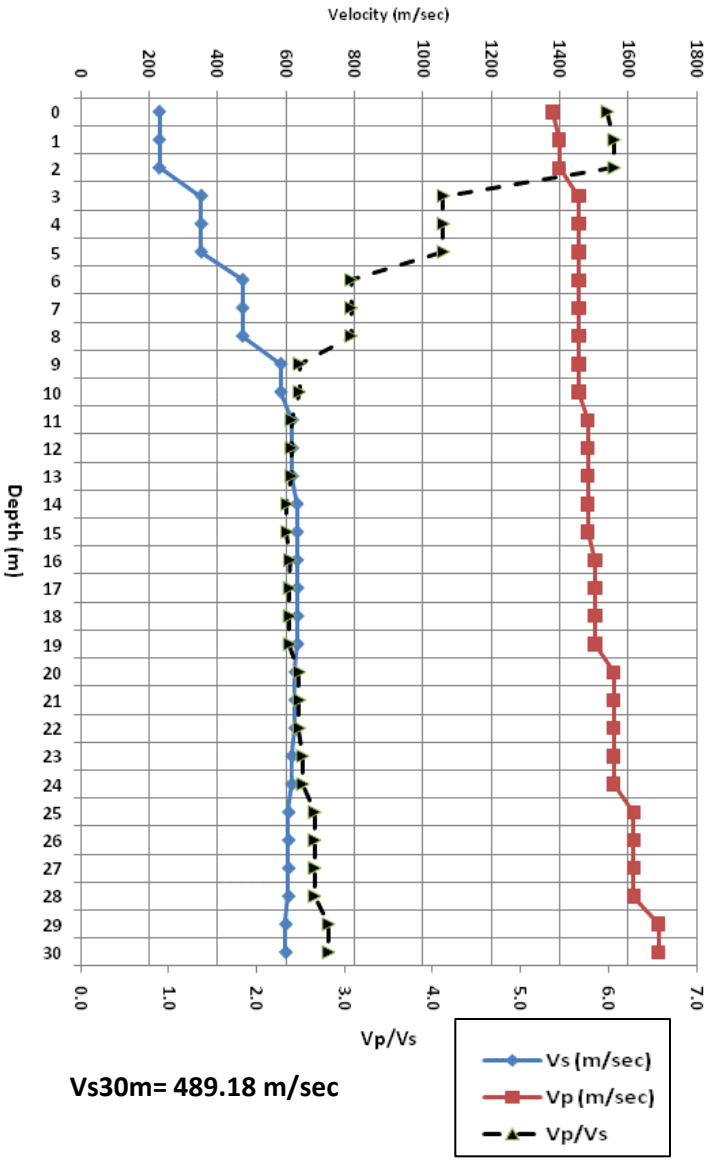

Vs30m= 489.18 m/sec

Figure A19. Vs, Vp, Vp/Vs and Poisson's Ratio profiles at UWFH.

WISH

Depth (meters)	Vs (downhole seismic) (m/sec)	Vp (downhole seismic) (m/sec)	Vp/Vs	Poisson's Ratio
0	141.82	265.38	1.87	0.30
1	141.82	489.72	3.45	0.45
2	236.59	805.12	3.40	0.45
3	236.59	1257.99	5.32	0.48
4	338.11	828.19	2.45	0.40*
5	477.62	836.23	1.75	0.26
6	477.62	2090.65	4.38	0.47
7	477.62	1331.47	2.79	0.43
8	559.17	1851.93	3.31	0.45
9	692.86	1697.15	2.45	0.40*
10	692.86	1215.40	1.75	0.26
11	734.92	2375.92	3.23	0.45
12	734.92	1398.40	1.90	0.31
13	734.92	1800.19	2.45	0.40*
14	734.92	1800.19	2.45	0.40*
15	734.92	1800.19	2.45	0.40*
16	766.72	1878.07	2.45	0.40*
17	766.72	1878.07	2.45	0.40*
18	766.72	1878.07	2.45	0.40*
19	701.66	1420.44	2.02	0.34
20	701.66	2473.73	3.53	0.46
21	723.72	1772.75	2.45	0.40*
22	723.72	1772.75	2.45	0.40*
23	723.72	1772.75	2.45	0.40*
24	723.72	1989.38	2.75	0.42
25	723.72	1990.41	2.75	0.42
26	803.91	1991.30	2.48	0.40
27	803.91	2486.82	3.09	0.44
28	803.91	1969.17	2.45	0.40*
29	803.91	1969.17	2.45	0.40*
30	803.91	1969.17	2.45	0.40*

**Interval P-wave velocities (Vp) are corrected based on the Vs and assumed Poisson's Ratio=0.40*

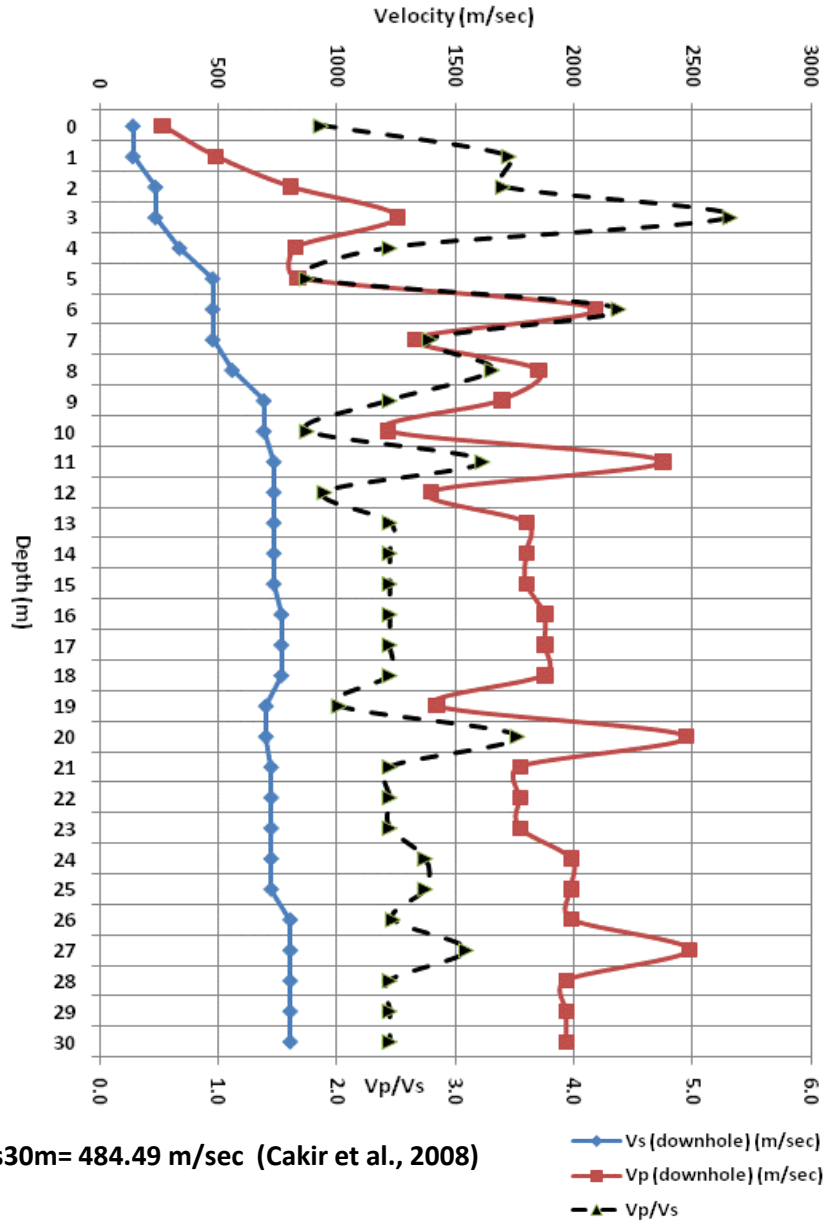

Vs30m= 484.49 m/sec (Cakir et al., 2008)

Figure A20. Vs, Vp, Vp/Vs and Poisson's Ratio profiles at WISH.